

# Journal of the Atmospheric Sciences

## Observations of the Development and Vertical Structure of the Lake Breeze Circulation During the 2017 Lake Michigan Ozone Study

--Manuscript Draft--

<b>Manuscript Number:</b>	JAS-D-20-0297
<b>Full Title:</b>	Observations of the Development and Vertical Structure of the Lake Breeze Circulation During the 2017 Lake Michigan Ozone Study
<b>Article Type:</b>	Article
<b>Abstract:</b>	<p>Ground-based thermodynamic and kinematic profilers were placed adjacent to the western shore of Lake Michigan at two sites as part of the 2017 Lake Michigan Ozone Study. The southern site near Zion, Illinois, hosted a microwave radiometer (MWR) and a sodar wind profiler, while the northern site in Sheboygan, Wisconsin, featured an Atmospheric Emitted Radiance Interferometer (AERI), a Doppler lidar, and a High Spectral Resolution Lidar (HSRL). Each site experienced several lake breeze events during the experiment. Composite time series and time/height cross sections were constructed relative to the lake breeze arrival time so that commonalities across events could be explored.</p> <p>The composited surface observations indicate that the initial post-breeze wind direction is consistently southeasterly at both sites regardless of pre-breeze wind direction. Surface relative humidity increases with the arriving lake breeze, though this is due to cooler air temperatures as absolute moisture content stays the same or decreases. The profiler observations show that the vertical structure of the lake breeze depends greatly on the local degree of thermodynamic instability: when unstable lapse rates are found in the lower troposphere, the lake breeze grows deeper and penetrates further inland than with stable lapse rates. The cold air associated with the lake breeze remains confined to the lowest 200 m of the troposphere even if the wind shift is observed at higher altitudes. The evolution of the lake breeze corresponds well to observed changes in baroclinicity and calculated changes in circulation. Collocated observations of aerosols and particulate matter show increases during the lake breeze as well.</p>

We would like to open our response with a note to all reviewers. During the course of revisions, we found that we had made a mistake in Figure 6, the figure that shows the relationship between stability, winds, and the degree of lake breeze front penetration. In brief, our plot did not properly reflect the classes to which a particular lake breeze was assigned (inland vs. near shore) for the Sheboygan cases. Since this is the data used to discuss the slope of the lake breeze with respect to penetration length, the previous discussion on this topic is no longer valid. Updated analysis concerning the interpretation of this figure can be found in Section 4c. This figure also featured an unusual bug in which part of some wind barbs were being cut off when being plotted. This made it appear that there were 50 kt winds when none were present. When remaking this figure, we thinned the number of barbs and made them larger to improve readability .

We regret the error, and thank you for your patience. We now turn to the point-by-point response to the reviewers:

\* \* \* \* \*

The authors have submitted a revised version of the manuscript that is a marked improvement over the original. However, there are unfortunately still fundamental problems. The majority of the results are still not novel (though some of the sampling technology and related analysis is), and the authors do not appear to have a full understanding of meteorological influences on the development and evolution of the lake breeze. They therefore misinterpret key findings that might have led to novel results.

I think there is some good data here with the potential for novel results, so I hope the authors will continue with improvements to the manuscript.

We appreciate that you feel we are making progress towards a publishable paper, and we hope that the further changes that we have made at your behest have further improved your opinion of our work.

Another problem - the LMOS 2017 overview paper that is referenced in the article has only been submitted to BAMS and therefore should not be used as a reference, nor can it be read by reviewers. It would be good to know how much overlap, if any, there is between this paper and the BAMS overview paper.

The BAMS overview paper has been accepted and is now available through early online release (<https://doi.org/10.1175/BAMS-D-20-0061.1>). We shared your concern about double-dipping on papers, and so we constructed both papers to cover separate topics. As a result there is very little overlap between the two papers, as the BAMS paper focuses on the experimental design, air chemistry, aircraft observations, and numerical modeling of ozone processes. The lake breeze is briefly discussed as a mechanism that influences ozone processes, but the composite analysis that is the basic framework upon which our manuscript is constructed is not

used at all. The wind profiling instruments are used in a single figure, Figure 7, to illustrate the evolution of the 2 June lake breeze event. That figure is reproduced here:

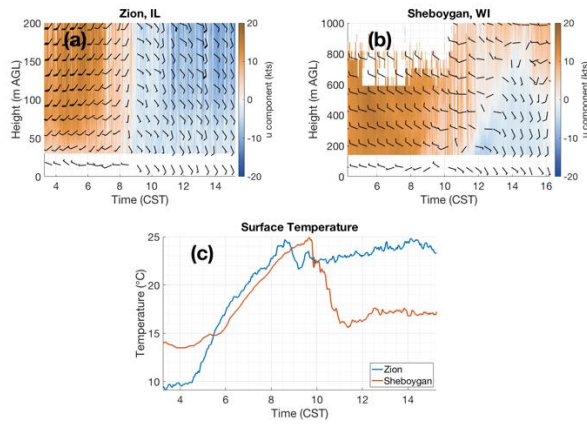


Figure 7. Winds (kts) observed by (a) sodar at Zion, Illinois and (b) Doppler lidar at Sheboygan, Wisconsin, and (c) surface air temperature (C) during the 2 June 2017 lake breeze event. Note the different vertical scale for the two wind cross sections.

The present paper does not focus on single cases while the BAMS paper only looks at this one case and does not investigate common characteristics across lake breezes. No thermodynamic profile observations are present in the BAMS paper. As far as air quality goes, the BAMS paper presents daily daytime PM 2.5 concentrations for every day of the experiment in one panel of one figure:

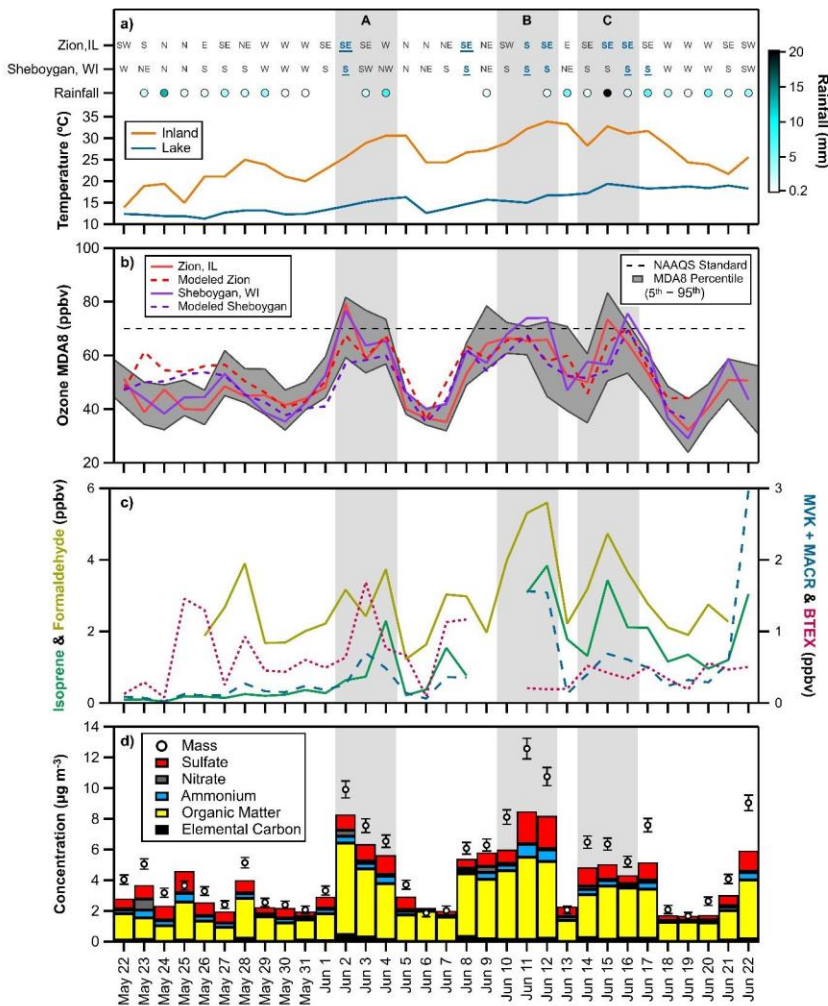


Figure 3. Observational overview of LMOS 2017. Shown are daily time series of (a) winds, rainfall and temperature, (b) ozone MDA8 concentrations, (c) peak hourly concentrations of selected gases, and (d) daytime PM2.5 concentrations and chemical composition. Grey vertical bands indicate ozone episodes. Figure notes: temperatures represent maximum hourly air temperature at Lake Mills, WI, and daily lake water temperature at Wilmette Buoy, IL; wind directions represent the most frequent wind direction during 0800–1600 CST (bold for lake breeze and underlined for deep inland penetration lake breeze); rainfall is the daily total averaged over 27 sites in WI and IL; Sheboygan ozone data are from the KA station; all variables for (c) and (d) are from Zion, IL, except formaldehyde is from the Sheboygan site; gas concentrations are peak hourly values for each day, and (d) is for daytime only (0700–1900 CST).

Again, the BAMS paper does not discuss the specific impacts of the lake breeze on these concentrations nor does it attempt to identify commonalities across lake breeze events as our

paper does. Therefore, we think these two papers are very complementary towards each other. While there is certainly overlap in the target audience for these papers, there is very little overlap in the content between them.

Overall, if the paper can be further improved, they should consider submission to a more applied meteorology journal such as the Journal of Applied Meteorology and Climatology, or Monthly Weather Review.

#### Detailed Comments

-----

L287 - Re "The lake breeze at Zion is much less effective at neutralizing the cross-shore temperature gradient...", the authors state here that there is a difference in the ability of the lake breeze at Zion to 'neutralize' the gradient, but in the next sentence they correctly point out that the lake air mass undergoes more modification at Zion due to its more inland location. Thus, this difference has little to do with how effective the lake breeze is at 'neutralizing' the temperature gradient (whatever that means).

You are correct, and we have reworded this sentence so that the change is no longer attributed directly to the lake breeze.

L298 - The amount of moisture available to be advected onshore by the lake breeze is a function of the air temperature of the marine air mass, and Table 2 shows that the lake temperatures at Sheboygan were 2-4C cooler than those at Zion. This likely explains at least some of the notable decreases in mixing ratio with LBA at Sheboygan, and should be investigated and reported on by the authors.

This was implied, but not very clearly. We have changed the wording to make this more explicit.

L305 - I had to read this line a few times to figure out its meaning. I suggest something like 'It is well known that the structure and influence of the lake breeze circulation extends vertically beyond the near-surface level.'

The suggested wording change has been made.

L343 - It appears to me that that there is warming between 200 and 300 m that is likely due to subsidence within the lake breeze circulation, creating a strong subsidence inversion over an already strong marine inversion. The authors should also mention that such a strong marine inversion is typical in spring when the lakes are still relatively cold.

Upon reading this critique, we looked at the vertical velocities from the Doppler lidar at Sheboygan. We agree that there is subsidence throughout this time, though it may be difficult to disentangle the circulation-based subsidence from the synoptic-scale subsidence that was

generally present throughout these cases. We have rewritten a portion of this paragraph to include these and other points, while addressing this and the next two comments.

L347 - It is not clear why cooling of the marine air mass via conduction needs to be invoked. The relatively low temperature of the marine air mass is mainly due to air around it having a relatively high temperature due to insolation, subsidence, or advection. Any cooling by conduction is a much slower process.

It is likely that air in contact with the lake surface is being cooled via conduction, with a small degree of cooling above the surface layer caused by heat being conducted into the surface layer (since there is very little mixing over the lake). That being said, when rewriting this section we removed the reference to conduction entirely.

L349 - I fail to see what the authors see here. Fig. 3 shows that the lake breeze (inflow layer) is roughly 220 m deep (i.e. below the inversion) in both cases, with both significant temperature and wind differences in that layer. Wind differences above that layer are likely due to the updraft and/or return flow branches of the circulation.

Again, this has been deleted when this section was rewritten.

L371 - The 'delay in the arrival' of lake-modified winds at higher levels is most likely due to the slope of the lake breeze front, which depends on the strength of the opposing synoptic-scale flow. As I commented in the first review, the synoptic-scale flow is important in that it can control both the slope of the lake-breeze front and the degree to which a lake breeze can penetrate inland. Looking at Fig. 3, it is clear that even in the composite there is a fairly strong opposing (west-northwesterly) flow found at Sheboygan, reaching 25 kt at 600 m just a couple of hours before LBA. This will generally cause the lake breeze circulation to take on a shallow wedge shape and retard its inland progress. Examples of this can be found in Mariani et al. 2018 and Curry et al. 2017 (in the authors' reference list), and also discussed in Simpson (1994, also in the authors' reference list).

This comment is related to the next one, and we are addressing both simultaneously below.

L476 - Re the degree of 'deepening', it is clear from Fig. 6 that the opposing flow is much greater for the near-shore cases than the inland cases, with composite winds at 600 m reaching up to 50 kt for the near shore cases versus up to 10 kt in the inland cases. Again, with such strong opposing flow, the lake breeze will not penetrate very far inland (if it penetrates inland at all) and the circulation will take on a shallow wedge shape. Thus the depth will increase very slowly with distance from the LBA location. Conversely, when there is weak opposing flow, the lake breeze can penetrate inland more easily and the depth of the inflow layer will increase more rapidly. It's not clear how this relates to the stability analysis that the authors perform, but this analysis should be revisited within the context of the synoptic flow.

Some of this comment has been addressed by our reformulation of Figure 6.

We agree that the lake-breeze front has a sloped interface and have added this to the revision as suggested. We believe our discussion of a perturbation horizontal pressure gradient force is complementary and provides a reasonable, dynamically-based explanation for the slope. Stronger westerly winds indicate a stronger synoptic-scale horizontal pressure gradient force. The momentum in this flow would result in a slower response to the additional onshore-directed perturbation horizontal pressure gradient force that develops and a shallower slope to the lake-breeze front. Unfortunately, the lidar data is missing for the span of time from LBA +1 to LBA +3 at Sheboygan for the sole near-shore case, so we are unable to fully assess the impact of near-shore vs. inland and stable vs. unstable on the slope of the lake breeze front.

L484 - Re hint of periodicity, this is likely remnant thermals in the convective boundary layer that has had the lake breeze slide beneath it. This was documented by Curry et al. 2017, for example.

We're not certain that this is what is being displayed here. Curry notes thermals on shorter time scales (on the order of 10 mins) than what we're seeing here (on the order of 1 h), and since we're averaging multiple cases together it seems unlikely that stochastically-generated thermals would align from one event to the next.

L491 - Given the above discussion, this explanation is unlikely.

Reference to the sloped interface has been added to the text.

L495 - Re lake breezes and aerosols, the authors should be aware of a paper by Davis et al. (2020).

We thank the reviewer for bringing this paper to our attention. Davis et al. (2020) is now cited in the paper. Its aerosol discussion focused on AOD trends and comparison of the AERONET and MAX-DOAS AODs at 361 nm. At the LMOS 2017 Zion site, an AERONET was co-located with in situ aerosols measurements (e.g. particle size distribution, calculated PM<sub>2.5</sub> from size distribution, and aerosol filter collection for mass and composition).

The AOD analysis methods from Davis et al (2020) could not be replicated in our current paper due to (a) less available AOD data from LMOS 2017, and (b) considerable differences in the sites themselves. Specifically: 1) The screened level 2 (L2) AOD data from AERONET was sparse during LMOS 2017 around the lake breeze arrival times, 2) LMOS 2017 lacked an additional AOD measurement such as MAX-DOAS. Additionally, the measurement site in Davis et al (York University) was 17 km north the Lake Ontario shoreline with the downtown of Toronto between the lake and measurement site. Zion site was located 1 km west of the Lake Michigan shoreline with no major emission sources between the lake and site. The difference in fetch, and in aerosol emissions and secondary aerosol precursor emissions between the lake and the observation sites in the two papers makes meaningful comparison difficult.

Both studies lacked highly temporal PM composition data. The integrated aerosol filters located at Zion do provide composition, but are an average of 12 hr periods. The unique measurement in this work is the highly temporal particle size distributions, which highlighted a significant increase in the ultrafine particle mode following the lake breeze arrival. The Davis et al paper did remind us of the important fact that AOD is wavelength dependent. Davis et al analyzed AOD at 361 nm, which is more sensitive to fine particles. The use of 550 nm AOD is most common within the satellite AOD community, and that is what we used in the previous version. In revision, we included AERONET AOD at both 361 nm and 550 nm. For our measurement period, which was rich in fine and ultrafine particles, we note that AOD at 380 nm can be double that of AOD at 550 nm.

Davis et al. analysis noted a decreasing trend in PM<sub>2.5</sub> while this work observed an increase in PM<sub>2.5</sub> concentrations following the onset of the lake breeze. For LMOS 2017, this increase was determined to be statistically significant by T-test and Wilcoxon Rank Sum Test at 95% significance level and  $p < 0.002$ .

L506 - 'After the growth in the depth of' should be 'After the depth of' or 'Once the depth of'

This has been addressed in the rewriting of this section.

L523 - How are aerosols 'processed'? Should be at least a sentence on this.

Based on further analysis completed while responding to reviewer comments and questions, this discussion of possible contribution factors has been updated to better reflect our current thoughts and understanding.

L533 - I would argue that only the thermodynamic analysis is unprecedented in detail.

The whole clause reads, “[t]he unique combination of kinematic and thermodynamic profilers at each site enables the analysis of lake breeze structure in unprecedented detail.” With no prior work combining high-temporal resolution wind and thermodynamic profilers, we are able to see how the thermodynamic structure evolves, and how the thermodynamic structure is related to the wind structure. The reviewer notes that the thermodynamic analysis is unprecedented, which means that the combination of wind and thermodynamics presented here is also unique to this work. Therefore, we feel that our phrasing here is correct.

L535-548 - This 'result' from the study is already well known. This needs to be removed and greater focus placed on novel results (when achieved).

This paragraph is the first part of a larger synthesis of the observations into a comprehensive picture of how the lake breezes evolved according to the observations examined here and sets up the following two paragraphs. We have augmented this section with greater emphasis on the thermodynamic profiler observations to highlight the role of this unique instrumentation in achieving this interpretation and we have more directly included the evolution of the aerosol in

this discussion to provide a more holistic picture of what our instruments are describing. Overall, however, we feel that this paragraph contributes significantly to the narrative.

L549 - I believe that the authors have shown that the lake breeze inflow layer is about 200 m deep. The lake breeze front is not really characterized, and would be considerably stretched downwind in the near-shore cases.

If a front is defined as a density discontinuity, then the depth of the lake breeze front is less than 200 m. If it is defined as the surface over which the wind shift is happening, then that reaches up to substantially higher altitudes. Here, we were basing this off of the depth of the initial impulse of onshore flow as observed by the Zion sodar. However, in certain cases it does rapidly grow to beyond that depth, so we have updated the language to say 100 – 200 m.

L561 - Be clear on what rises.

The original wording could have implied that the cold lake air was rising. We have reworked this sentence to improve its clarity, and we thank you for bringing it to our attention.

Fig. 1 - should be 'lack of convective cloud adjacent to the lake shore'

This change has been made.

\* \* \* \* \*

Reviewer #3: The authors made great efforts to address the reviewers' concerns and comments, and the revised version is largely improved as compared to the previous submission. Overall, the revised manuscript is well written.

Thank you for your appreciation of our efforts thus far. We hope that we have been able to address your remaining concerns to your satisfaction.

However, several points require further clarification or improvement.

1. Impact on aerosols (Section 5). The authors use two of nine figures (Fig.8-9) but relatively short pages to discuss the impact of lake breezes on aerosols. In-depth analyses or detailed discussions on this are not sufficient. For instance, the number concentrations of aerosols show a sharp increase in the diameter range of 20-80 nm. To me, this is the most attractive point or interesting finding from all of the figures presented in this study. In fact, the authors have pointed out this on Lines 513-515, but possible reasons accounting for such a large increase are not discussed. In addition, what heights does the top panel represent since I do not see a large increase in the mean concentrations of PM<sub>2.5</sub> near surface (bottom panel in Fig.9)?

We thank the reviewer for interest in the aerosol discussion. We have expanded the discussion of these aerosol-related figures somewhat. We should clarify that all aerosols presented in Figure 9 were measured at the surface, 5 m AGL. The top panel of Figure 9 is a two dimensional representation of three dimensional data. Using a common convention in the aerosol science community, in Figure 9, the x-axis is time, the y-axis is particle diameter, and the z-axis (color) is the intensity of the number size distribution function at a specific time and particle size. It should be noted that the color scale is logarithmic.

A more conventional plot of the before and after size distribution function is shown here. The large increase in 20-80 nm particles can be seen more quantitatively in this plot. The average mode in the size distribution post-LBA was 38 nm, or in the Aitken mode, and tend to have a short lifetime (minutes to hours) as they quickly grow into larger aerosols. These ultrafine aerosols have very small masses and thus do not impact the PM<sub>2.5</sub> mass concentrations.

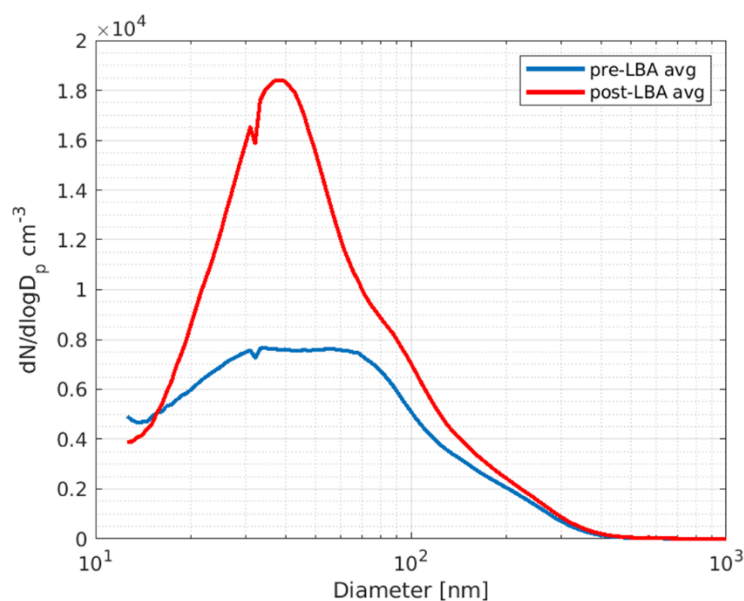


Figure. Average of 3 hr pre-LBA (blue) and 3 hr post-LBA (red) for aerosol size distributions for lake breeze event days.

There are many possible reasons for the source of increase in the ultrafine aerosols between 20-80 nm size range that include:

- small number of lake breeze days for analysis leading to statistical noise in the analysis
- ultrafine aerosols from gas-to-particle nucleation and/or primary nuclei mode emissions (e.g., combustion sources) followed by growth in size and decrease in number from coagulative scavenging and condensational growth.
- Lake spray aerosols produced by wave breaking events over Lake Michigan (Slade et al. 2010, now in manuscript reference list)

- Ultrafine aerosols have a tendency to peak around noon leading to increased ultrafine particles in lake breezes (which arrive slightly before midday) relative to air masses at Zion earlier in the day.

To quantify the contributing factors, or even rank them, would require more events, high temporal ultrafine and fine PM composition, and/or more measurements over the lake.

In addition, the authors do not mention anything on this work (Section 5) in the conclusion section even though it isn't the center of this study.

We have augmented the existing synthesis of the cycle of lake breeze development presented in the conclusions with the state of aerosol concentrations at the appropriate times.

2. Section 4 is the heavy part of the manuscript. It contains 9 pages and major contents. My reading feels a little bit tired. I would like to suggest splitting it into several sub-sections with each section being focused on one topic. This is a suggestion but not required.

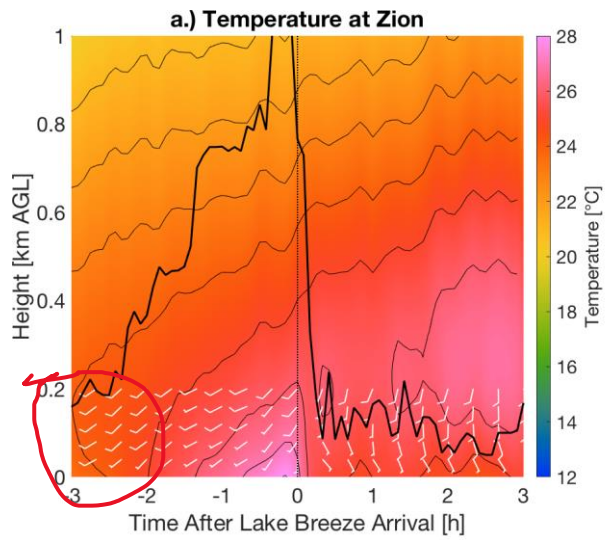
This is a good suggestion. Until you mentioned this, we were not aware just how long Section 4 was and that we hadn't included any breaks. Were it to be published in this format, there would be multiple pages of wall-to-wall text and most readers would be fatigued. We have added the following section breaks: a. Temperature and Moisture Structure; b. Baroclinicity and Circulation; c. Inland Penetration and Low Level Structure.

3. L36-37: The last sentence of the abstract is not informative and confused. What is the difference between "aerosols" and "particulate matter"? What "increases" do you mean here? mass or number concentrations?

We have edited the last sentence of the abstract and updated the manuscript to be more clear of when we discuss particle number concentrations vs particulate matter (particle mass concentration).

4. L330-331: I do not see an evident inversion layer before LB arrives in Figs.3a and 3c, 6a and 6c. Please correct me if I misunderstood it.

We reworked the first part of that sentence to say "There is an inversion present a few hours before LBA" to help clarify that we don't mean immediately before LBA. By looking at the contour lines in the lower-left corner of Fig. 3a (highlighted below) a weak inversion can be seen; it is admittedly quite difficult to see when relying on the colors alone. Fig. 3c displays moisture content and would not necessarily be indicative of an inversion. The inversion is more readily visible in Fig. 6, again hours before LBA instead of immediately before.



5. L476: "In the hours that follow" is not complete.

We inadvertently placed a period where we meant to have a comma. This has been corrected. Thank you for your attention to detail.

1     **Observations of the Development and Vertical Structure of the Lake Breeze Circulation**  
2                                   **During the 2017 Lake Michigan Ozone Study**

3     Timothy J. Wagner<sup>1</sup>, Alan C. Czarnetzki<sup>2</sup>, Megan Christiansen<sup>3</sup>, R. Bradley Pierce<sup>1,4</sup>, Charles O.  
4                                   Stanier<sup>3</sup>, Angela F. Dickens<sup>5</sup>, and Edwin W. Eloranta<sup>1</sup>.

5             1. Cooperative Institute for Meteorological Satellite Studies (CIMSS), Space Science and  
6             Engineering Center (SSEC), University of Wisconsin – Madison, Madison, Wisconsin

7             2. Department of Earth and Environmental Sciences, University of Northern Iowa, Cedar Falls,  
8                                   Iowa

9             3. Department of Chemical and Biochemical Engineering, University of Iowa, Iowa City, Iowa

10            4. Department of Atmospheric and Oceanic Science, University of Wisconsin – Madison,  
11                                   Madison, Wisconsin

12            5. Lake Michigan Air Directors Consortium (LADCO), Rosemont, Illinois

13

14

15     Corresponding author: Timothy J. Wagner, tim.wagner@ssec.wisc.edu

16

17

18 **Abstract**

19           Ground-based thermodynamic and kinematic profilers were placed adjacent to the western  
20 shore of Lake Michigan at two sites as part of the 2017 Lake Michigan Ozone Study. The southern  
21 site near Zion, Illinois, hosted a microwave radiometer (MWR) and a sodar wind profiler, while  
22 the northern site in Sheboygan, Wisconsin, featured an Atmospheric Emitted Radiance  
23 Interferometer (AERI), a Doppler lidar, and a High Spectral Resolution Lidar (HSRL). Each site  
24 experienced several lake breeze events during the experiment. Composite time series and  
25 time/height cross sections were constructed relative to the lake breeze arrival time so that  
26 commonalities across events could be explored.

27           The composited surface observations indicate that the initial post-breeze wind direction is  
28 consistently southeasterly at both sites regardless of pre-breeze wind direction. Surface relative  
29 humidity increases with the arriving lake breeze, though this is due to cooler air temperatures as  
30 absolute moisture content stays the same or decreases. The profiler observations show that the lake  
31 breeze penetrates deeper when the local environment is unstable and pre-existing flow is weak.  
32 The cold air associated with the lake breeze remains confined to the lowest 200 m of the  
33 troposphere even if the wind shift is observed at higher altitudes. The evolution of the lake breeze  
34 corresponds well to observed changes in baroclinicity and calculated changes in circulation.  
35 Collocated observations of aerosols show increases in number and mass concentrations after lake  
36 breeze passage.

37

38 **1. Introduction**

39

40 It is well known that the Laurentian Great Lakes have a significant impact on the weather  
41 and climate of the upper Midwestern United States. These large bodies of water (which  
42 collectively encompass approximately 18% of the world's supply of liquid freshwater) force  
43 changes in temperature, cloud cover, and precipitation with significant diurnal and seasonal  
44 variability (Scott and Huff 1996), and the impacts of the lakes can even extend to severe convective  
45 weather (King et al. 2003). The lake breeze circulation is one of the most important mechanisms  
46 for latent and sensible heat exchange between the lakes and the surrounding environment. This is,  
47 in part, due to common occurrence of the Great Lakes lake breezes. For example, Laird et al.  
48 (2001) constructed a 15-year climatology of Lake Michigan lake breeze events and found that lake  
49 breezes tended to occur more frequently as the summer progressed. Depending on the location,  
50 lake breeze frequency increased from 5 to 9 events per month in May to 8 to 12 per month in  
51 August. Other studies have used different criteria to identify lake breezes and found higher  
52 frequencies. Lyons (1972) showed that Chicago, Illinois, experienced a lake breeze on  
53 approximately half of all days in May through September. With events occurring multiple times  
54 a week during the warm months, operational forecasters need to be familiar with their formation,  
55 structure, and impacts, while numerical weather prediction and air quality models must be able to  
56 simulate them properly.

57 Since a substantial fraction of the world's population lives in coastal regions, sea and lake  
58 breezes have been a subject of interest to humanity since antiquity (Simpson 1994, Miller 2003)  
59 and the broad outlines of their formation have been known for generations. Due to water's large  
60 heat capacity, its ability to absorb solar energy over a finite depth, and the vertical mixing present

61 in large bodies of water, surface temperatures respond slowly to solar heating. On the seasonal  
62 timescale, peak lake surface temperatures lag their terrestrial counterparts by several weeks while  
63 on diurnal scales lake temperatures are typically colder than land during the day but warmer at  
64 night. As a result, a sharp land-water gradient in the temperature and density of the near-surface  
65 air can arise, inducing a circulation as the atmosphere attempts to restore equilibrium. This  
66 circulation is commonly found where the body of water has sufficient thermal mass relative to the  
67 land. While the sea breeze and Great Lakes breezes are well known, lake breezes have also been  
68 observed for both natural lakes and reservoirs with length scales of just a few km (Segal et al.  
69 1997).

70 A robust solenoidal-based explanation of the lake breeze circulation has emerged (Holton  
71 1992, Miller et al. 2003, Martin 2006). The Bjerknes circulation theorem states that the material  
72 (Lagrangian) change in the absolute circulation  $C_a$  of a fluid element can be described as:

73

$$\frac{dC_a}{dt} = - \oint \frac{dP}{\rho} \quad (1)$$

74

75 where  $P$  is pressure and  $\rho$  is density. In the special case of a barotropic fluid, density is a function  
76 of pressure alone and the right-hand side reduces to the closed line integral of an exact differential  
77 (which is zero). Thus, Bjerknes's circulation theorem is merely a more general case of Kelvin's  
78 circulation theorem, which states that the absolute circulation in a barotropic fluid is conserved.  
79 However, the differential heating present at a lake or sea boundary ensures that the environment is  
80 far from barotropic: the daytime geopotential heights are greater over the land, and thus isobars  
81 slope downward toward the cooler water while isopycnals (lines of constant density) slope toward  
82 warmer land. This ensures that the **environment** is baroclinic. The horizontal flow both at the

83 surface and aloft is isobaric and does not contribute to the circulation change, as  $dp = 0$  for those  
84 branches. However, as the daytime ascending branch (over land) and the descending branch (over  
85 water) are associated with environments with very different densities, there is a net difference  
86 between these two branches and thus an acceleration along the perimeter of the fluid element is  
87 induced. This is a thermally direct circulation, and over time the vertical motions would be  
88 expected to reduce the baroclinicity of the environment as the isopycnals would be rotated to be  
89 more parallel to the isobars. At night, a weak land breeze can develop when the temperature  
90 gradient is reversed.

91 Changes in the thermodynamic structure of the environment would clearly be expected to  
92 accompany the changes in the kinematics described above. The development of onshore flow at  
93 low levels produces cold air advection. The flow of this comparatively denser air from water to  
94 land takes the form of a localized gravity current (Miller et al. 2003). The cooler air inhibits  
95 convection, producing clearing skies that can be seen on satellite imagery; a characteristic example  
96 of this is depicted in Figure 1. Since temperatures above the gravity current are not affected, a  
97 shallow inversion will develop (Keen and Lyons 1978).

98 The present study comprehensively describes the temporal and vertical development of the  
99 lake breeze circulation on the western shore of Lake Michigan using data collected during the 2017  
100 Lake Michigan Ozone Study (LMOS 2017, Stanier et al. 2021). The development and structure of  
101 western Lake Michigan breezes have been of considerable interest for many (e.g. Lyons 1972,  
102 Keen and Lyons 1978, Sills et al. 2011), likely due in part to the large population centers located  
103 along the lake shore. One aspect of the relationship between these major urban areas and the lake  
104 is the adverse impacts that lake breezes have on air quality, as they have been shown to play a  
105 significant role in the production and transport of ground-level ozone in shoreline communities

106 along Lake Michigan (Lyons and Cole 1976, Dye et al. 1995, Levy et al. 2010). Ozone precursors  
107 emitted from densely populated regions are transported over the lake. So long as the precursors  
108 remain offshore, the shoreline communities are not impacted by increased ozone production.  
109 When the lake breeze is present, however, ozone and its precursors are transported inland and  
110 convergence along the lake breeze boundary results in significant increases to observed ozone  
111 concentrations. The deployment of high-temporal resolution thermodynamic and kinematic  
112 profilers alongside aerosol lidars, air samplers, and other instruments, at two sites adjacent to Lake  
113 Michigan in support of LMOS 2017, allows the investigation of lake breeze events from a novel  
114 perspective. While other studies have investigated the kinematic characteristics of lake and sea  
115 breezes using higher-temporal resolution profiling instruments like Doppler lidars (e.g., Curry et  
116 al. 2017, Banta et al. 1993) and sodars (e.g., Mastrantonio et al. 1994, Prakash et al. 1992), the  
117 present work introduces continuous thermodynamic profiling using instruments observing both  
118 microwave and infrared emission. When coupled with collocated wind profiling instruments, a  
119 detailed picture of the thermodynamic and aerosol characteristics of the lake breeze circulation  
120 and its evolution emerges. Wind and thermodynamic profiles from lake breeze events are  
121 composited on an event-centric time scale to capture the behavior of the atmosphere before and  
122 after lake breeze arrival; a similar technique has been used to investigate the near-storm  
123 environment of severe storms (Wagner et al. 2008) and bores (Loveless et al. 2019). The  
124 remainder of this paper describes the field campaign and the instruments (Section 2), explores the  
125 evolution of surface weather conditions (Section 3), vertical structure (Section 4), and particulate  
126 air quality (Section 5), and synthesizes these observations to improve understanding of lake breeze  
127 circulations from the combined thermodynamic and kinematic perspective (Section 6).

128

## 129 **2. Measurements and Instrumentation**

### 130 *a. The 2017 Lake Michigan Ozone Study*

131           The 2017 Lake Michigan Ozone Study (LMOS 2017) was devoted to observing chemical  
132 and meteorological features important to persistently high ozone concentrations along the western  
133 edge of Lake Michigan. Project collaborators included NASA, NOAA, EPA, the Lake Michigan  
134 Air Directors Consortium (LADCO), state environmental agencies, universities, and the private  
135 sector. A significant goal of LMOS 2017 was to better understand how the unique geography and  
136 meteorology of the Lake Michigan basin drives significant ground-level ozone production even in  
137 communities with relatively low emission rates of ozone precursors. By uniting land-based, ship-  
138 based, and airborne measuring systems, a comprehensive portrait of the thermodynamic,  
139 kinematic, and chemical state of the coastal environment during high ozone events was obtained.  
140 An additional goal of the experiment was to use the data to evaluate the performance of  
141 meteorological and air quality models and inform their improvement.

142           The field phase of LMOS 2017 was conducted from 22 May to 22 June 2017. This period  
143 historically encompasses a significant number of ozone exceedance events for shoreline  
144 communities due to the combination of numerous lake breeze events (as the lake has not yet  
145 warmed significantly) coupled with sufficient insolation to induce the photochemistry required for  
146 ground level ozone production; the cold water also inhibits mixing and ensures that precursors  
147 remain near the surface. Two ground-based supersites were established. The more southerly  
148 supersite was near Zion, Illinois (roughly halfway between Chicago and Milwaukee). The northern  
149 supersite was at Sheboygan, Wisconsin (about 80 km north of Milwaukee); a map depicting their  
150 locations is seen in Figure 1. The Sheboygan site (43.745 N, 87.709 W) was within 230 m of the  
151 shore while the Zion site (42.468 N, 87.810 W, AQS 17-097-1007) was approximately 1 km

152 inland. The lake shore has a similar north-south orientation in the vicinity of the two sites, although  
153 the shoreline is more sinuous at Sheboygan. In-depth descriptions of the two sites are found in  
154 Doak et al. 2021. Airborne platforms included the NASA UC-12, which carried remote sensing  
155 instruments for aerosols, clouds, and trace gases, and a light aircraft operated by Scientific  
156 Aviation, which conducted in situ profiling of trace gases and meteorological characteristics. The  
157 NOAA research vessel R5503 provided near-shore transects of surface meteorology and trace gas  
158 concentrations with a Pandora differential absorption optical spectrometer (Herman et al. 2009),  
159 while on-shore vehicles conducted mobile sampling of terrestrial ozone and meteorology.  
160 Preliminary campaign results have been reported (Abdioskouei et al. 2019, Vermeuel et al, 2019)  
161 and analysis of this significant volume of data is ongoing.

162

### 163 *b. Instrumentation*

164 For the purposes of the present work, the most significant data were collected at the two  
165 supersites near Sheboygan and Zion. The Space Science and Engineering Center (SSEC) Portable  
166 Atmospheric Research Center (SPARC, Wagner et al. 2019) was deployed at Sheboygan, while a  
167 Radiometrics MP3000 and an Atmospheric Systems Corporation acoustic wind profiler, or sodar,  
168 were deployed at Zion. Surface observations at the two sites came from instruments mounted on  
169 10 m towers, and each site also featured air quality instrumentation to measure ozone and  
170 particulate matter.

171 SPARC, a portable ground-based atmospheric profiling laboratory, includes an  
172 Atmospheric Emitted Radiance Interferometer (AERI, Knuteson et al. 2004a, 2004b), a Halo  
173 Photonics Stream Line XR Doppler lidar (DLID, Pearson et al. 2009), and a High Spectral  
174 Resolution Lidar (HSRL, Shipley et al. 1983, Eloranta 2005). The thermodynamic state is captured

175 by AERI, a commercially-available hyperspectral infrared radiometer that passively measures  
176 downwelling near- and thermal infrared spectra with a spectral resolution better than  $1 \text{ cm}^{-1}$  and a  
177 temporal resolution of approximately 30 s. Profiles of temperature and water vapor can be  
178 retrieved from AERI-observed spectra through the Tropospheric Remotely Observed Profiling via  
179 Optimal Estimation (TROPoe) retrieval, formerly known as AERIOe (Turner and Löhnert 2014,  
180 Turner and Blumberg 2019). TROPoe profiles have been shown to agree well with radiosondes  
181 when they originate from either an AERI (Turner and Löhnert 2014, Turner and Blumberg 2019)  
182 or an MWR (Turner and Löhnert 2021). The a priori atmospheric state for the retrieval during this  
183 deployment was calculated from a multiyear climatology of late spring and early summer  
184 radiosondes launched from the National Weather Service office at Green Bay, Wisconsin. A  
185 principal component analysis noise filter is applied to the AERI radiances to reduce noise before  
186 the retrieval is applied, in which the observations are decomposed into principal components and  
187 the spectrum is rebuilt from those that have the greatest variance (Turner et al. 2006). The DLID  
188 uses a  $1.5 \text{ }\mu\text{m}$  pulsed laser to capture the radial velocity of boundary layer aerosols; by scanning  
189 at a fixed zenith angle at different azimuths, it is possible to geometrically calculate the wind  
190 profile above the lidar. The HSRL is a vertically-pointing lidar that uses spectral width differences  
191 to discriminate between molecular and aerosol scattering: the spectrum for aerosol backscattering  
192 is confined to the relatively narrow range of Doppler-shifted frequencies associated with vertical  
193 motions in the atmosphere while the molecular spectrum is broadened by the Maxwellian thermal  
194 motion of the molecules. This allows high-precision absolutely-calibrated aerosol backscatter  
195 retrievals and independent retrievals of aerosol extinction. With these instruments, SPARC is able  
196 to provide a comprehensive profile of the evolution of the atmospheric state on a time scale that is  
197 measured on the order of minutes.

198 At Zion, the MWR passively observed the brightness temperature of downwelling radiance  
199 in 22 channels. Eight channels between 22.234 and 30.000 GHz measure the water vapor  
200 absorption band and 14 channels between 51.248 and 58.800 GHz observe the oxygen absorption  
201 band. The TROPoe algorithm was then used to retrieve profiles of water vapor and temperature  
202 from these measurements using the same prior data as were used for the Sheboygan retrievals; by  
203 using TROPoe instead of the manufacturer-supplied neural network retrievals, a more direct  
204 comparison to the AERI observations at Sheboygan could be carried out. The sodar operates at  
205 audio frequencies near 4500 Hz, emitting a high intensity acoustic pulse and sampling the  
206 atmospheric echo from that pulse. The acoustic antenna is an array of 32 speakers that are used to  
207 both transmit and receive signals. The speaker array is electrically steered to generate a set of three  
208 independent pulses. The frequency of each resulting echo is directly proportional to the radial  
209 motion of the scattering volume relative to the antenna. The radial motions determined from the  
210 Doppler shift of each pulse in a set are combined to produce three-dimensional wind profiles from  
211 30 to 200 m above ground level (AGL).

212 The Zion site was also home to several air quality instruments. A Scanning Mobility  
213 Particle Sizer and Aerodynamic Particle Sizer (SMPS-APS, Shen et al. 2002) system measured  
214 aerosol size distributions at the surface, covering a combined aerodynamic diameter size range of  
215 13 nm – 8354  $\mu\text{m}$ . The size distributions from the APS were converted from aerodynamic to  
216 electrical mobility diameters (SMPS) and merged to the final size distribution following the  
217 method presented in Khlystov et al. (2004). Size distributions were averaged to a common 10-min  
218 time series. An Aerosol Robotic Network (AERONET, Holben et al. 1998) measuring aerosol  
219 optical depth (AOD) was also located at the Zion site from June 4 – June 22 of the campaign.

220 AERONET level 2.0 data (cloud screened and quality assured) are used in the present work  
221 (Smirnov et al. 2000). AOD was interpolated to 550 nm in the following manner:

$$222 \quad \tau_{\lambda_{550}} = \tau_{\lambda_{500}} \left( \frac{\lambda_{550}}{\lambda_{500}} \right)^{-\alpha} \quad (2)$$

223 where  $\tau_{\lambda_{500}}$  is AOD at 500 nm and  $\alpha$  is angstrom exponent (440-870 nm) as reported by  
224 AERONET. The relevant characteristics of the instruments used in this study are summarized in  
225 Table 1.

226

### 227 c. Lake breeze events

228 The following criteria were used to objectively identify the lake breeze events (defined as  
229 the passage of a lake breeze front) at the two sites:

- 230 1. The zonal (u) component of the surface wind reversed from offshore to onshore.
- 231 2. Surface temperatures dropped abruptly with the wind shift.
- 232 3. Mixing height decreased with the wind shift.
- 233 4. No rain was detected within three hours of the wind shift.

234 Laird et al. (2001) identified a set of criteria to objectively identify lake breeze, including a change  
235 in wind direction, maximum air temperatures greater than that of the lake surface, and synoptically  
236 quiescent conditions. While the Laird et al. (2001) criteria were not specifically used as filtering  
237 criteria in the present study, all of the lake breeze events examined here also satisfied these criteria.

238 The identification criteria were applied separately to the Sheboygan and Zion observations,  
239 and the time of the lake breeze arrival (LBA), representing the moment the lake breeze front passed  
240 over the observing sites, was defined as the time of the greatest shift in wind direction. This  
241 resulted in a total of six lake breeze events at each location, consistent with the climatology for  
242 late spring (Laird et al. 2001). Five study days included lake breeze at both sites. The remaining

243 two lake breeze events occurred at one supersite but not the other. On average, LBA occurred  
244 much earlier at Sheboygan (1541 UTC, 10:41 AM local time, 9:41 AM LST) than Zion (1630  
245 UTC, 11:30 AM local time, 10:30 AM LST). However, the small number of cases and variability  
246 in arrival times at each site means this difference is not statistically significant. For the five days  
247 in which lake breezes were observed at both locations, the correlation in LBA was low ( $r=0.0935$ ).  
248 The lack of correlation between arrival times is consistent with an understanding that lake breeze  
249 events are driven more by local conditions than by synoptic forcing. Analysis of contemporaneous  
250 surface maps helps illustrate this last point: in all cases, any synoptic scale disturbances were either  
251 hundreds of km removed from the observing sites, were stationary, or did not propagate over the  
252 observation domain until after the period analyzed in this paper. The dates and times of the  
253 observed lake breezes are shown in Table 2.

254

### 255 **3. Composite Surface Conditions**

256 An objective method to identify the timing of lake breeze events was used to composite  
257 the individual cases observed during the LMOS 2017 campaign. For each event, the time of LBA  
258 was subtracted from the observation times so that the resulting timeline was measured relative to  
259 LBA. The observations from each instrument and event were then interpolated to a common  
260 timeline with 5 min resolution from 3 h before LBA to 3 h after; this facilitated comparisons across  
261 instruments and events. Figure 2 illustrates the results of this composite analysis for the surface  
262 conditions at the two sites. Results from Sheboygan (Zion) are shown with solid (dashed) lines.  
263 Thin colored lines represent individual events while thick black lines represent the mean of all  
264 events for a particular site. The mean wind speed and direction were calculated by first determining  
265 the mean zonal ( $u$ ) and meridional ( $v$ ) components of the wind, then converting to speed and

266 direction. Overall, surface conditions are consistent with what would be expected during a lake or  
267 sea breeze event, but there are some interesting details. Panel 2a exhibits the wind directions for  
268 the various events, with the wind shift used to define LBA clearly evident. Both sites have nearly  
269 identical time series for the mean wind direction, with westerly winds undergoing a rapid shift to  
270 southeasterly at LBA followed by a much slower turning towards a more southerly direction over  
271 the ensuing hours, a result of Coriolis (inertial) acceleration. Substantial variations from one event  
272 and site to the next can be seen prior to LBA, but once the lake breeze front has passed the wind  
273 directions are much more uniform. This lower variability in wind direction may be due to  
274 consistency in the onshore perturbation horizontal pressure gradient force that develops as the air  
275 over land warms, and the reduced friction surface winds experience flowing over water. The wind  
276 speed (Figure 2b) shows substantial variability between cases and from one time step to the next.  
277 On average, the speeds are higher at Zion than Sheboygan, and while Sheboygan has little change  
278 in the mean wind speed pre- and post-LBA, the mean winds at Zion are over 1.4 times faster after  
279 LBA than they were before.

280         While the driving factor of the lake breeze circulation is the difference between the  
281 temperatures of the air over land and water, the lack of observations of the latter means that the  
282 lake surface temperature needs to be used as a proxy. Figure 2c shows the time series for the  
283 difference between the air and lake temperature on lake breeze days. In situ observations of the  
284 lake temperature are sparse, with no operational buoys within tens of km of Sheboygan. Therefore,  
285 lake surface temperatures were obtained from the Great Lakes Research Laboratory (GLERL)  
286 Great Lakes Surface Environmental Analysis (GLSEA, Schwab et al. 1999). Values were obtained  
287 from the GLSEA grid points located approximately 10 km from the observation sites at an azimuth  
288 of 140 degrees (the average wind direction 1 h after LBA). The analyses are computed once per

289 day, and these temperatures are recorded in Table 2. On average, the lake at Zion is about 3 °C  
290 warmer than near Sheboygan, and during the month-long experiment seasonal warming caused a  
291 greater increase at Zion. On average the air/lake temperature difference (Figure 2c) gradually but  
292 steadily increases at a rate that is effectively identical for both locations. Following LBA, the mean  
293 lake/land difference decreases substantially at Sheboygan, dropping from 12.2 °C at LBA to 3.2  
294 °C just one hour later. A smaller change is observed at Zion, as the mean air/lake temperature  
295 difference goes from 12.1 °C to 9.7 °C during the same period. The overall pattern for ambient  
296 air temperature is largely the same as the air/lake differences (not shown). Air temperatures at Zion  
297 tended to be warmer than at Sheboygan both before and after LBA, a function of Zion's lower  
298 latitude, a longer fetch over land to reach the observing site, and lake breezes that occurred later  
299 in the day allowing more solar heating before LBA. Absolute water vapor content (as represented  
300 by the mixing ratio, Figure 2d) shows a very gradual increase in the hours before LBA consistent  
301 with typical evolution of the planetary boundary layer (PBL). The lake breeze itself has very little  
302 impact on the mixing ratio at Zion for any event, but four of the six Sheboygan events experience  
303 a notable decrease in mixing ratio with LBA. This can be explained by the relative differences  
304 between the lake air and land air temperatures at the two sites: Zion had a much smaller difference  
305 than Sheboygan, so there was little difference between the saturation mixing ratios following LBA.  
306 By contrast, Sheboygan experienced a significant decrease in its saturation mixing ratio following  
307 LBA, and so absolute water vapor content decreased even though the arriving air originated over  
308 a large body of water. By contrast, the relative humidity at both sites (not shown) showed an  
309 increase following LBA. Since the absolute humidity was constant or decreasing following LBA,  
310 this increase in relative humidity was solely driven by the decrease in air temperature.  
311

#### 312 **4. Composite Vertical Structure**

313           It is well known that the structure and influence of the lake breeze circulation extends  
314 vertically beyond the near-surface level. Previous studies have used frequent balloon launches  
315 (Lyons 1972), instrumented aircraft (Finkele 1995), and kinematic profilers (e.g. Curry et al. 2017,  
316 Banta et al. 1993) to investigate the vertical structure of lake breeze circulations. However,  
317 continuous contemporaneous observations of winds, temperature, and moisture profiles during  
318 lake and sea breeze events have been rare. LMOS 2017 provided a unique opportunity to assess  
319 how the vertical structure of these fields evolved over time during several different lake breeze  
320 events. Here, the same compositing technique described earlier is applied to the vertical dimension  
321 so that structure in the PBL can be resolved. An important caveat when looking at the vertical  
322 plots of remotely-sensed thermodynamic variables is that the true vertical resolution (that is, the  
323 minimum size of an element that can be resolved by the profiler) is finer for an infrared than a  
324 microwave radiometer due to the narrower weighting functions and higher information content  
325 found in the infrared band (Ebell et al. 2013, Blumberg et al. 2015). The TROPoe retrieval can be  
326 used to quantify how well each instrument resolves both temperature and water vapor structure.  
327 On average, at the 200 m level (which is roughly the height of the post-LBA inversion), the AERI  
328 vertical resolution for temperature was approximately twice as fine as the MWR (0.25 km and 0.49  
329 km respectively) and was approximately 2.5 times better for water vapor (1.19 km and 3.00 km  
330 respectively). Therefore, the enhanced detail visible in the Sheboygan time-height cross sections  
331 of thermodynamic variables is far more likely to be due to the differences in the instruments used  
332 than physical differences in the lake breeze itself.

333

334 *a. Temperature and Moisture Structure*

335 Time-height cross sections of temperature and mixing ratio overlaid with wind barbs are  
336 shown in Figure 3. Observations from all instruments were interpolated onto a common grid with  
337 temporal resolution of 5 min (same as the surface composites shown earlier) and a vertical spacing  
338 of 20 m. The data from both Zion and Sheboygan illustrate that while the increase in temperature  
339 in the period leading up to LBA is greatest at the surface, increases in temperature with time are  
340 seen several hundred meters above the surface as the surface air is mixed upward. There is an  
341 inversion present a few hours before LBA that is more easily seen in Sheboygan than Zion. There  
342 are two reasons for this: first, since the average time of LBA is earlier at Sheboygan, the three-  
343 hour period preceding LBA is more likely to include an early-morning inversion; and second,  
344 enhanced vertical resolution enables the AERI to resolve the inversion with increased fidelity.  
345 Prior to LBA winds near the surface are southwesterly and are veering with height, becoming  
346 northwesterly at an altitude of 1 km. Wind direction at a given height tends to be constant with  
347 time before LBA, though there is a tendency for the speeds to decrease with time. In the 30 min  
348 prior to LBA, the potential temperature gradient in the lowest 400 m (not shown) is greatly relaxed  
349 as the lower troposphere undergoes significant mixing while the free troposphere remains largely  
350 adiabatic both before and after LBA. The arrival of the lake breeze brings with it a sudden decrease  
351 in temperature that is greatest at the surface but still prevalent in the lowest 100 – 200 m; again,  
352 this is more evident in the AERI observations. A strong inversion develops post-LBA as the cold  
353 lake air advances beneath and lifts the warmer land air. Strong marine inversions such as these  
354 are expected in the spring when the lakes are significantly colder than the nearby land. Above the  
355 inversion, the air temperature at a given height increases with time. This is likely subsidence-  
356 induced warming, caused by the descending branch of the lake breeze circulation, which helps to  
357 enhance the strength of the inversion and increase the stability of the environment. Therefore, the

358 cold temperatures commonly associated with the lake breeze are confined to a shallow layer in the  
359 lowest part of the troposphere even as the breeze-induced changes in wind direction extend above  
360 that height. Figure 3 also shows the mixing height calculated from the composited thermodynamic  
361 profiles. Mixing height grows throughout the morning with increased diabatic heating, and is  
362 deeper at Zion where air temperatures are warmer. However, the arrival of the lake breeze causes  
363 a sudden drop in the mixing height as the atmosphere rapidly stabilizes. This has significant  
364 ramifications on air quality, as the lake breeze circulation-induced inversion causes ozone  
365 precursors and other pollutants to be trapped in the near-surface air (Dye et al. 1995, Levy et al.  
366 2010).

367         These observations show a disconnect between the depth of cold air and the depth over  
368 which the lake breeze circulation is impacting wind direction. The depth of the cold air that arrived  
369 onshore is limited by the vertical extent of conductive cooling. Both observations and numerical  
370 simulations indicate that significant heat loss by conduction is limited to the lowest 150 m of the  
371 atmosphere (Lyons 1970). However, winds are clearly changing above the cold pool. Before LBA,  
372 westerly surface winds indicate the synoptic scale horizontal pressure gradient force is directed  
373 toward the northeast. With sunrise, the near-surface air over land warms more rapidly with solar  
374 heating, producing a perturbation horizontal pressure gradient force directed onshore. In  
375 combination with the synoptic scale horizontal pressure gradient force, this produces an  
376 ageostrophic southeasterly surface wind at LBA. Observations over land indicate the warming  
377 eventually continues above the cold layer, but is delayed after collapse of the mixed layer resulting  
378 from LBA at the surface. It is likely this upper warming over land is greater than above the  
379 lake. As a result, the onshore perturbation horizontal pressure gradient force also develops at upper

380 levels, but later than at the surface. Therefore, one would expect a delay in the arrival of  
381 southeasterly winds at higher levels and a gradual upward slope to the advancing lake breeze front.

382 Vertical profiles of the water vapor mixing ratio are also displayed in Figure 3. It can be  
383 challenging to interpret remotely-sensed profiles of moisture as the information content present in  
384 the infrared and microwave spectra for moisture is less than for temperature. Consequently, the  
385 vertical distribution of water vapor is not as clearly resolved as is temperature. Due to these  
386 limitations it is likely that vertical gradients in moisture are actually greater than what is shown.  
387 Still, valuable insight can be obtained by inspecting the observations. Mixing ratio profiles at  
388 Sheboygan show markedly lower values than at Zion, which is consistent with the surface  
389 observations. However, due to the lower temperature at Sheboygan, the relative humidity values  
390 (not shown) are of similar magnitude at the two sites. In the hours before LBA, warming-induced  
391 evaporation likely explains the observed increase in mixing ratio; simultaneously, the relative  
392 humidity is constant/decreasing with time as the effect of increased water vapor on relative  
393 humidity is outpaced by the higher temperatures. Following LBA, the mixing ratio observations  
394 in the lowest level of the profiles at the two sites are consistent with the values reported by the  
395 surface observations: nearly constant at Zion and slightly decreasing at Sheboygan.

396 The sodar and Doppler lidar are clearly resolving the lower branch of the lake breeze  
397 circulation. What is not clearly evident in these figures, however, is the presence of the upper  
398 level return flow. While the 200 m vertical range of the Zion sodar is likely too shallow,  
399 conceivably the lidar at Sheboygan could observe it since aircraft observations of a sea breeze by  
400 Finkle et al. (1995) showed return flow occurring between 700 and 1000 m. With easterly surface  
401 winds at Sheboygan post-LBA one would expect corresponding westerly winds aloft that would  
402 augment the existing westerly flow, in which case the winds aloft would increase following LBA.

403 However, Figure 3 clearly shows that for the composite lake breeze presented here the westerly  
404 flow actually decreases in magnitude following LBA. An examination of the individual u wind  
405 components for each of the cases shows that the 12 June case may exhibit return flow above 1.25  
406 km; the other cases do not have lidar observations at that height due to a lack of sufficient aerosol  
407 scattering on those days. Lyons (1972) showed return flow for Chicago-area lake breezes tended  
408 to peak around 1500 m AGL. Therefore, the return flow in these cases may simply be beyond the  
409 range of the lidar.

410

#### 411 *b. Baroclinicity and Circulation*

412 Time/height cross sections of pressure and density can be seen in Figure 4. Since there are  
413 not corresponding high-temporal resolution profiles over the lake, a definitive characterization of  
414 the baroclinicity of the environment cannot be made. However, the rate at which density changes  
415 relative to pressure can inform as to how quickly the environment is becoming more or less  
416 baroclinic. At the start of the analysis period, the isopycnals are parallel to isobars at all observed  
417 levels at Sheboygan, but daytime heating causes the density to change more quickly than the  
418 pressure. At Zion, the isobars and isopycnals are already intersecting at the start of the analysis,  
419 but the later LBA time means more heating has taken place. Below 300 meters at Sheboygan (and  
420 throughout the entire depth of observations at Zion), the isopycnals slope downward in the  
421 time/height cross section meaning that the atmosphere is becoming less dense with time as it  
422 approaches LBA. At the same time, close inspection of Figure 4 shows a slight upward slope in  
423 the isobars compared to the horizontal lines of the altitude grid. Once the lake breeze arrives, the  
424 slope of the isopycnals with respect to time reverses sign as the atmosphere rapidly becomes more  
425 dense with the arrival of the cold, dry air. After approximately one hour, the isopycnals and isobars

426 are parallel again, which is consistent with a barotropic atmosphere. The density of the lake breeze-  
427 advected air is greater at Sheboygan than it is at Zion, behavior that is expected given the disparity  
428 in temperatures between the two locations. When combined, the profiling observations at  
429 Sheboygan and Zion are consistent with the solenoidal characterization of lake breeze circulations  
430 described earlier. It is important to note that the TROPoe retrieval algorithm derives the  
431 thermodynamic variables on a height grid and then calculates the pressure hypsometrically which  
432 assumes that the atmosphere is in hydrostatic balance. While the small horizontal scale of sea  
433 breezes means that they do not necessarily behave hydrostatically, numerical modeling studies  
434 (e.g. Yang 1991) indicate that there is little difference between hydrostatic and nonhydrostatic  
435 simulations of weak sea breezes. Therefore, any error in the isobars in Figure 4 due to a lack of  
436 hydrostatic balance is likely to be small.

437         The role of pressure and density in generating a lake breeze can be further explored by  
438 using Equation 1 to calculate how the thermodynamic state at a given time forces changes in the  
439 circulation with time. Results using the composite AERI profiles at Sheboygan integrated over  
440 several different depths of the atmosphere are shown in Figure 5. Regardless of the integration  
441 depth, the rate of change of circulation before LBA is close to zero or slightly negative. However,  
442 there is a substantial increase in the circulation rate at 0 h LBA, coincident with the observed shift  
443 in surface winds. This increase is visible at all analyzed heights, though the value for the 20 m  
444 layer is less than half of the values for the deeper layers. The values for 100 m and 200 m depth  
445 are neutral to positive for 1.5 h after LBA, which indicates that the lake breeze circulation  
446 continues to intensify after the time of LBA, coincident with the continued turning of the winds as  
447 observed by the DLID during that period. Altogether, these data are consistent with the theory that  
448 the lake breeze is actually a change in circulation that arises from local density differences. The

449 observations at Zion (not shown) did not indicate similar behavior, although this is more likely an  
450 artifact of the coarse vertical resolution of the MWR rather than a product of any atmospheric  
451 difference at Zion.

452

### 453 *c. Inland Penetration and Low Level Structure*

454 One of the ways in which individual lake breeze events differ is the degree to which they  
455 penetrate inland. Certain lake breezes remain near-shore, impacting the conditions only within a  
456 few hundred meters of the shore or less, while others can extend hundreds of kilometers inland.  
457 To investigate the role of vertical structure on inland penetration, the events were classified into  
458 “near-shore” or “inland” based on observed winds at inland sites. These inland observations came  
459 from two air quality monitoring sites operated by the Wisconsin Department of Natural Resources:  
460 Kenosha Water Tower, 5.7 km inland from the shore and 15 km northwest of Zion; and Sheboygan  
461 Haven, 5.3 km inland from the shore and 10 km northwest of Sheboygan. The locations of these  
462 sites relative to the Zion and Sheboygan supersites are marked on Figure 1. If an observed wind at  
463 the inland site experienced a shift in wind direction that was consistent with the lake breeze for 3  
464 h or more, it was considered to represent an inland lake breeze event. Based on these criteria, three  
465 of the six events at Zion were classified as inland events while all but one event at Sheboygan were  
466 classified as such; these events are identified in Table 2 in bold type. To assess what, if any, role  
467 instability may have had in the penetration distance of the lake breezes, data from the AERI and  
468 MWR profilers were used to calculate the vertical rate of change of equivalent potential  
469 temperature  $\theta_e$ . Results are displayed in Figure 6. Positive (negative) values for  $d\theta_e/dz$ ,  
470 representing convectively stable (unstable) conditions, are shaded in red (blue). While the small  
471 sample size makes it difficult to draw definitive conclusions, at least for the events observed here,

472 the inland lake breeze cases tended to form in more unstable environments (as evidenced by the  
473 blue shading above the near-surface layer) than the near-shore cases (which have more pink  
474 shading in the lowest 500 m). This is an interesting finding that stands in contrast to theory  
475 (Rotunno 1983, Walsh 1974), which states that the length scale of inland penetration of sea breezes  
476 is proportional to stability. However, modeling studies (e.g. Xian and Pielke 1991) have found that  
477 more unstable environments produce lake breezes with deeper penetrations. The Doppler lidar  
478 observations at Sheboygan indicate some correspondence between the strength of the pre-existing  
479 westerly flow and whether a lake breeze penetrates inland or not, as the pre-LBA winds aloft in  
480 the sole near-shore case (12 June 2017) are stronger than the mean winds aloft of the inland cases.  
481 This is consistent with findings by Curry et al. (2017) and Mariani et al. (2018), who note that  
482 stronger offshore winds hinder the inland progression of the lake breeze front. It may be that the  
483 preexisting flow, not the local convective stability, is the most important parameter for determining  
484 the degree of penetration. Doppler lidar observations at Sheboygan for the single near-shore case  
485 were absent for most of the post-LBA period. As a result, this study is unable to fully address the  
486 relative importance of stability versus wind speed in determining the degree of inland penetration.

487         The Zion sodar has a fine vertical resolution (10 m) and narrow dead band at the surface  
488 (30 m), and so it is well-suited for investigating the structure of the lake breeze in greater detail.  
489 Figure 7 shows the time-height cross section of the mean zonal ( $u$ ) and vertical ( $w$ ) components  
490 of the sodar-observed winds during both the inland and near-shore cases; recall that there is an  
491 identical number (3) of events of each type at Zion. Since the shoreline at Zion is oriented in a due  
492 north-south direction, the  $u$  component of the wind effectively represents the cross-shore flow and  
493 a switch in the sign from positive to negative represents passage of the lake breeze front. It is  
494 clear from the results that, regardless of breeze type, the lake breeze front is a near-vertical wall

495 approximately 100 m deep that arrives right at LBA and disrupts the predominately westerly flow.  
496 In the hours that follow, the near-shore cases exhibit little deepening from that initial impulse as  
497 the negative values for  $u$  remain limited to the lowest 100 m of the troposphere. The inland cases,  
498 however, quickly show growth in the depth of the system to at least double their initial height. As  
499 noted above, the inland cases formed in more unstable environments. However, the  
500 contemporaneous vertical velocity observations indicate that thermodynamic instability is not  
501 likely to be the reason for the discrepancy in the two breeze types as the magnitudes of the vertical  
502 motion are largely similar during and following LBA for both breeze types. The strongest vertical  
503 lifting is found right at LBA as the arriving cold air acts as a density current and displaces the  
504 shoreline air upward. Following LBA, there is a hint of periodicity in the upward motion,  
505 especially in the near-shore (stable) cases where positive vertical velocities are seen starting 30  
506 min after LBA with a frequency of approximately 1 h. It is unlikely that these structures are  
507 thermals embedded in the convective boundary layer [as documented by Curry et al. (2017)] as  
508 these are occurring on a longer time scale and are the result of multiple cases being averaged  
509 together. The inland (unstable) cases tend towards more pronounced periods of vertical lift  
510 following LBA. However, these times are not well-correlated with the vertical growth of the  
511 onshore flow. In fact, the lake breeze experiences its greatest vertical extent at the same time that  
512 the atmosphere is undergoing its most consistent period of subsidence. This tends to rule out  
513 momentum advection due to thermodynamic instability as a cause for growth of the lake breeze  
514 layer. Since the MWR observations indicate that the cold pool is not deepening with time, a more  
515 likely solution is that an onshore perturbation horizontal pressure gradient force has developed  
516 aloft, producing a sloped interface along the advancing lake breeze front.  
517

## 518 5. Aerosol Impacts

519 The HSRL deployed at Sheboygan allows for the observation of absolutely-calibrated  
520 profiles of aerosol backscatter. Molecular backscattering often obscures the contributions of  
521 aerosols in traditional backscatter lidars, but the HSRL technique is able to separate and remove  
522 molecular scattering from the observed backscatter. During two of the six lake breezes observed  
523 at Sheboygan, enhanced aerosol backscatter was observed by the HSRL at the same altitude and  
524 time as the Doppler lidar observed the wind shift. These two cases can be seen in Figure 8, which  
525 shows the time/height cross section of the base-10 logarithm of the aerosol backscatter cross  
526 section. In both cases (and in other cases not presented here) the growth of the boundary layer with  
527 solar heating can be seen as the increasing depth over which enhanced backscatter is visible  
528 starting before LBA but continuing after; this is especially apparent in the 2 June case in which  
529 the growth is easily visible starting nearly 3 h before LBA. After the growth in the depth of the  
530 lake breeze is significant enough that it can be observed by the Doppler lidar, both cases show  
531 additional enhanced backscatter coincident with the shifting wind barbs, though it is more subtle  
532 on 2 June than 16 June. This is consistent with the lake breeze containing, on average, a slight  
533 enhancement in fine aerosols.

534 Increases in fine and ultrafine aerosol number concentrations were also observed around  
535 the time of LBA at Zion. Figure 9a shows the aerosol size distribution while Figure 9b shows the  
536 times series of **particulate matter with aerodynamic diameter less than 2.5 micron (PM<sub>2.5</sub>)**. In the  
537 composite average, aerosols at sizes of 20-80 nm increase dramatically at the time of LBA. Similar  
538 graphs made for non-lake breeze days (not shown) do not show the 20-80 nm enhancement. The  
539 mean quantitative increase in the total aerosol number is from 8413 cm<sup>-3</sup> (pre LBA) to 12,435 cm<sup>-3</sup>  
540 (post LBA), and was statistically significant using a two-sample t-test. At the size where the post-

541 LBA feature is most notable (38 nm), the size distribution function increases in height by a factor  
542 of 2.7.

543 Changes in other aerosol variables at Zion were investigated as well, including aerosol  
544 optical depth, integrated aerosol volume, and PM<sub>2.5</sub>. As shown in Figure 9b, for the 3 h period  
545 before LBA to the 3 h period after LBA, PM<sub>2.5</sub> increased by 2.5 µg m<sup>-3</sup> on lake breeze days. This  
546 increase was greater than the increase on non-lake breeze days (0.6 µg m<sup>-3</sup>); for non-lake breeze  
547 days, the average LBA time at Zion was used as the time to determine the relative difference. This  
548 difference was found to be statistically significant using a two-sample t-test (p=0.02). In situ  
549 integrated aerosol volume increased as well, consistent with the increases in aerosol number and  
550 PM<sub>2.5</sub>. The increases in aerosol volume and PM<sub>2.5</sub> were not as distinct at the time of LBA as the  
551 change in ultrafine aerosol number, but rather suggested increasing mass of secondary aerosol in  
552 the air coming off the lake at later times in the day.

553 AOD at 550 nm on lake breeze days (not shown) ranged from approximately 0.03 to 0.22,  
554 and AOD at 331 nm ranged from approximately 0.08 to 0.43. However, the AOD data were too  
555 sparse to create a composite time series or inspect for discontinuities at the LBA time. In a study  
556 in Toronto, increases in AOD and surface and vertical column density NO<sub>2</sub> were observed at LBA  
557 time (Davis et al. 2020), but direct comparisons cannot be drawn due to differences in land use,  
558 nearby sources, and fetch of the observation sites.

559 The general conceptual model of lake breeze pollution episodes in the region (Dye et al.  
560 1995), supported by LMOS 2017 results in Hughes et al. (2021) and Doak et al. (2021), suggest  
561 that much of the aerosol signal seen after LBA is due to anthropogenic pollution from land-based  
562 sources within the Lake Michigan airshed. Oxidation of precursor species leads to secondary  
563 aerosol formation in these plumes that are transported over the lake and then returned in the lake

564 breeze. The conceptual model explains the gradual increase in aerosol volume and PM<sub>2.5</sub> seen after  
565 LBA, and the greater increase (afternoon vs. morning) on lake breeze days vs. non-lake breeze  
566 days. However, the conceptual model does not explain the distinct increase in ultrafine aerosol  
567 seen at the LBA time. This is consistent with ultrafine aerosols generating from breaking of  
568 freshwater waves (Slade et al. 2010, Axson et al. 2016); however, combustion sources over the  
569 lake, gas-to-particle nucleation over the lake (likely in land-based anthropogenic plumes), and  
570 other potential sources are possible. Other observations such as time-resolved measurements of  
571 wave state, ultrafine aerosol chemistry, and vertical profiles of aerosols would be required to  
572 elucidate specific contributions.

573

574

575

## 576 **6. Synthesis and Conclusions**

577 As part of the 2017 Lake Michigan Ozone Study, ground-based supersites were deployed  
578 at two locations adjacent to the western shore of Lake Michigan. The unique combination of  
579 kinematic and thermodynamic profilers at each site enables the analysis of lake breeze structure in  
580 unprecedented detail, and a compelling portrait of the development of this phenomenon emerges  
581 from the synthesis of these instruments and surface measurements.

582 These observations show that lake breezes during LMOS 2017 developed as follows. In  
583 the absence of synoptic forcing, a preexisting inversion can be found over the land in the overnight  
584 hours with predominately westerly flow throughout the lower troposphere. Background aerosol  
585 concentrations show little difference from average values during this time of the year. Following  
586 sunrise, several significant changes begin to take place in the lower troposphere. Over the next

587 three to four hours solar heating increases the surface temperature and the depth of the PBL while  
588 increased mixing erodes the previous inversion; analysis of the potential temperature profiles (not  
589 shown) indicates that the lower PBL becomes largely isentropic with height during this time.  
590 While the air over land warms, the lake temperature remains largely unchanged. As a result, the  
591 density of the air over land becomes much less than over water, which results in sloping isopycnals  
592 as observed by the thermodynamic profilers and an increase in baroclinicity. Since the change in  
593 the circulation around a fluid element is a function of the **magnitude** of the baroclinicity, a  
594 circulation in the vertical plane develops that is superimposed over the pre-existing westerly flow.  
595 Up to this point, there is little change in the winds as the preexisting circulation in the vertical  
596 plane is small. However, the baroclinic forcing results in a sudden increase in the circulation which  
597 manifests itself as the lake breeze. The change in circulation derived from baroclinicity is well-  
598 captured by the ground-based profilers.

599         The lake breeze front is on the order of 100 - 200 m deep and represents the leading edge  
600 of the air that has been cooled by conduction of heat into Lake Michigan. This air mass is advected  
601 over the land by the lower branch of the lake breeze circulation, and as it advances it forces an  
602 updraft that the wind profilers indicate is on the order of 1-2 m s<sup>-1</sup>. The concentration of aerosols  
603 having a diameter of 20 – 80 nm increases to nearly an order of magnitude above background  
604 levels with passage of the lake breeze front. While the change in PM<sub>2.5</sub> concentration is not as  
605 dramatic, it still shows a marked increase after the lake breeze front. The low level relative  
606 humidity over land increases with the passage of the lake breeze front, even as the absolute  
607 humidity is steady or even decreasing, owing to the significant decrease in temperature. Changes  
608 in the local thermodynamics result in decreased baroclinicity in the lower troposphere, and the

609 lake breeze circulation achieves a steady state within a few minutes with little change in wind  
610 speed or direction observed in the lowest 100 m after that time.

611 The local near-surface environment has been generally stabilized by the lake breeze as  
612 evidenced by strong increases in potential temperature with height in the lowest 100 - 200 m. The  
613 advancing cold air undercuts the warm air over land and lifts it, creating a strong inversion on the  
614 order of 8 K over just 200 m. While the aforementioned lifting can force cloud development along  
615 the lake breeze front, the strong stabilization of the atmosphere behind the front results in clearing  
616 skies, as seen in the satellite imagery in Figure 1.

617 Some questions remain about the reasons behind the different characteristics observed at  
618 the two sites. For example, the difference between the air and lake temperatures is nearly identical  
619 between the two sites in the period leading up to LBA, but there is substantial divergence in the  
620 temperature differences following LBA as the ensuing gradient is twice as strong at Zion as at  
621 Sheboygan. At the same time, the absolute moisture content of the air at Zion seems to be  
622 unaffected by the lake breeze while it drops by nearly half at Sheboygan. It is important to  
623 remember that there are slight differences in the set of cases used for analysis, as both the coldest  
624 day pre-LBA at Sheboygan and the warmest day post-LBA at Zion were the two event days on  
625 which there was no corresponding breeze at the other site. This would help bias the respective  
626 sites in opposite directions. The two sites themselves are not situated identically, either, as the  
627 Sheboygan site was much closer to the shore than the Zion site (230 m vs. 1 km). The longer fetch  
628 at Zion combined with the relatively slow speed at which lake-cooled air is advected over the  
629 warmer land means that the air can undergo substantially more modification at that site than  
630 Sheboygan. The degree of urban development also provides an interesting contrast between the  
631 two sites. At the microscale, the Sheboygan site was more urbanized as it was deployed next to a

632 resort development while the Zion site was within a state park. However, the community of  
633 Sheboygan is a discrete smaller city surrounded by farmland while Zion is in the heart of the urban  
634 amalgamation that lies between Chicago and Milwaukee. The degree to which these different  
635 settings may be impacting the characteristics of the lake breeze is an important question, but one  
636 that is beyond the scope of the present work.

637         For future studies of lake or sea breeze structure, an ideal site would contain both a sodar  
638 and a Doppler lidar so that a more complete profile of winds over the lowest kilometer of the  
639 atmosphere could be observed as the sodar would fill in all but the very lowest level of the lidar's  
640 dead band. When coupled with an AERI and in situ surface meteorology sensors, this would  
641 provide a near-continuous profile of atmospheric thermodynamics and kinematics from the surface  
642 to the maximum effective range of the lidar.

643

#### 644 **Acknowledgements**

645         The authors are indebted to David Turner, who assisted with applying the TROPoe  
646 algorithm to the microwave radiometer data. Steve Smith assisted with deployment of the  
647 radiometer and sodar at Zion while Erik Olson led the deployment of SPARC at Sheboygan. David  
648 Loveless and Coda Phillips (University of Wisconsin – Madison) and Jack Bruno (Ohio  
649 University) monitored the SPARC. Funding for the SPARC trailer deployment and the University  
650 of Northern Iowa's participation at Zion during LMOS 2017 was provided by the GOES-R  
651 Program Office via the NOAA Cooperative Agreement with the Cooperative Institute for  
652 Meteorological Satellite Studies (NA15NES432001). The three anonymous reviewers contributed  
653 many insightful comments and suggestions that greatly improved this paper. This work was funded

654 in part by the National Science Foundation under Grant AGS-1712909, AGS-1713001, and AGS-  
655 1712828.

656

### 657 **Data availability statement**

658 Profiler data used in this study are freely available from the LMOS 2017 campaign archive at  
659 <https://www-air.larc.nasa.gov/missions/lmos/index.html>. Inland wind observations were obtained  
660 from the EPA Air Quality System at <https://aqs.epa.gov/aqs/>.

661

### 662 **References**

663

664 Abdioskouei, M., Z. Adelman, J. Al-saadi, T. Bertram, G. Carmichael, M. Christiansen, P. Cleary,  
665 A. Czarnetzki, A. Dickens, M. Fuoco, M. Harkey, L. M. Judd, D. Kenski, D. Millet, R. B.  
666 Pierce, C. Stanier, B. Stone, J. Szykman and T. Wagner (2019). 2017 Lake Michigan  
667 Ozone Study (LMOS) Preliminary Finding Report. Available at  
668 [https://www.ladco.org/wp-](https://www.ladco.org/wp-content/uploads/Research/LMOS2017/LMOS_LADCO_report_revision_apr2019_final.pdf)  
669 [content/uploads/Research/LMOS2017/LMOS\\_LADCO\\_report\\_revision\\_apr2019\\_final.p](https://www.ladco.org/wp-content/uploads/Research/LMOS2017/LMOS_LADCO_report_revision_apr2019_final.pdf)  
670 [df](https://www.ladco.org/wp-content/uploads/Research/LMOS2017/LMOS_LADCO_report_revision_apr2019_final.pdf)

671 Axson, J. L., N. W. May, I. D. Colon-Bernal, K. A. Pratt and A. P. Ault, 2016: Lake spray aerosol:  
672 a chemical signature from individual ambient particles. *Environ. Sci. Technol.*, **50**, 9835-  
673 9845.

674 Banta, R. M., L. D. Olivier, and D. H. Levinson, 1993: Evolution of the Monterey Bay sea-breeze  
675 layer as observed by a pulsed Doppler lidar. *J. Atmos. Sci.*, **50**, 3959 – 3982.

676 Blumberg, W. G., D. D. Turner, U. Löhnert, and S. Castleberry, 2015: Ground-based temperature  
677 and humidity profiling using spectral infrared and microwave observations. Part II: actual  
678 retrieval performance in clear-sky and cloud conditions. *J. Appl. Meteor. Climatol.*, **54**,  
679 2305 – 2319.

680 Clough, S. A., M. W. Shepard, E. J. Mlawer, J. S. Delamere, M. J. Iacono, K. Cady-Pereira, S.  
681 Boukabara, and P. D. Brown, 2005: A summary of the AER codes. *J. Quant. Spectrosc.*  
682 *Radiat. Transfer*, **91**, 233-244.

683 Curry, M., J. Hanesiak, S. Kehler, D. M. L. Sills, and N. M. Taylor, 2017: Ground-based  
684 observations of the thermodynamic and kinematic properties of lake-breeze fronts in  
685 southern Manitoba, Canada. *Bound.-Lay. Meteor.*, **163**, 143 – 159.

686 Davis, Z. Y. W., D. M. L. Sills and R. McLaren, 2020: Enhanced NO<sub>2</sub> and aerosol extinction  
687 observed in the tropospheric column behind lake-breeze fronts using MAX-DOAS.  
688 *Atmos. Environ.*, **5**, 100066.

689 Doak, A. G. and coauthors, 2021: Characterization of ground-based atmospheric pollution and  
690 meteorology sampling stations during the Lake Michigan Ozone Study 2017. *J. Air Waste*  
691 *Manag. Assoc.*, **71**, 866 – 889.

692 Dye, T. S., P. T. Roberts, and M. E. Korc, 1995: Observations of transport processes for ozone and  
693 ozone precursors during the 1991 Lake Michigan Ozone Study. *J. Appl. Meteor.*, **34**, 1877  
694 – 1889.

695 Ebell, K., E. Orlandi, A. Hünerbein, U. Löhnert, and S. Crewell, 2013: Combining ground-based  
696 with satellite-based measurements in the atmospheric state retrieval: Assessment of the  
697 information content. *J. Geophys. Res. Atmos.*, **118**, 6940 – 6956.

698 Eloranta, E.W., 2005: High spectral resolution lidar. *Lidar: Range-Resolved Optical Remote*  
699 *Sensing of the Atmosphere*, K. Weitkamp, Ed. New York: Springer-Verlag, pp. 143–163.

700 Finkele, K., J. M. Hacker, H. Kraus, and R. A. D. Byron-Scott, 1995: A complete sea-breeze  
701 circulation cell derived from aircraft observations. *Bound.-Layer. Meteor.*, **17**, 299 – 317.

702 Herman, J., A. Cede, E. Spinei, G. Mount, M. Tzortziou, and N. Abuhassan, 2009: NO<sub>2</sub> column  
703 amounts from ground-based Pandora and MFDOAS spectrometers using the direct-sun  
704 DOAS technique: Intercomparisons and application to OMI validation. *J. Geophys. Res. -*  
705 *Atmos.*, **114**, doi: 10.1029/2009JD011848.

706 Holben, B. N. and coauthors, 1998. AERONET—A federated instrument network and data archive  
707 for aerosol characterization. *Remote Sens. Environ.*, **66**, 1-16.

708 Holton, J., 1992: *An Introduction to Dynamic Meteorology*, third ed., San Diego: Academic Press,  
709 511 pp.

710 Hughes, D. D., and coauthors, 2021: PM<sub>2.5</sub> chemistry, organosulfates, and secondary organic  
711 aerosol during the 2017 Lake Michigan Ozone Study. *Atmos. Environ.*, **244**, 117939.

712 Keen, C. S. and W. A. Lyons, 1978: Lake/land breeze circulations on the western shore of Lake  
713 Michigan. *J. Appl. Meteor.*, **17**, 1843 – 1855.

714 King, P. W. S., M. J. Leduc, D. M. L. Sills, N. R. Donaldson, D. R. Hudak, P. Joe, and P. B.  
715 Murphy, 2003: Lake breezes in southern Ontario and their relation to tornado climatology.  
716 *Wea. Forecasting*, **18**, 795 – 807.

717 Knuteson, R. O. and coauthors, 2004a: Atmospheric Emitted Radiance Interferometer. Part I:  
718 Instrument design. *J. Atmos. Oceanic Technol.*, **21**, 1763 – 1776.

719 Knuteson, R. O. and coauthors, 2004b: Atmospheric Emitted Radiance Interferometer. Part II:  
720 Instrument performance. *J. Atmos. Oceanic Technol.*, **21**, 1777 – 1789.

721 Laird, N., D. R. Kristovich, X.-Z. Liang, R. W. Arritt, and K. Labas, 2001: Lake Michigan lake  
722 breezes: Climatology, local forcing, and synoptic environment. *J. Appl. Meteor.*, **40**, 409  
723 – 424.

724 Levy, I., P. A. Makar, D. Sills, J. Zhang, K. L. Hayden, C. Mihele, J. Narayan, M. D. Moran, S.  
725 Sjostedt, and J. Brook, 2010: Unravelling the complex local-scale flows influencing ozone  
726 patterns in the southern Great Lakes of North America. *Atmos. Chem. Phys.*, **10**, 10895 –  
727 10915.

728 Loveless, D. M., T. J. Wagner, D. D. Turner, S. A. Ackerman, and W. F. Feltz, 2019: A composite  
729 perspective on bore passages during the PECAN campaign. *Mon. Wea. Rev.*, **147**, 1395 –  
730 1413.

731 Lyons, W. A., 1970: Numerical simulation of Great Lakes summertime conduction inversions.  
732 *Proc. 13th Conf. Great Lakes Res.*, Intl. Assoc. Great Lakes Res., 369-387.

733 Lyons, W. A., 1972: The climatology and prediction of the Chicago lake breeze. *J Appl, Meteor.*,  
734 1259 – 1270.

735 Lyons, W. A and H. S. Cole, 1976: Photochemical oxidant transport: mesoscale lake breeze and  
736 synoptic-scale aspects. *J. Appl. Meteor.*, **15**, 733 – 743.

737 Mariani, Z., A. Dehghan, P. Joe and D. Sills, 2018: Observations of lake-breeze events during the  
738 Toronto 2015 Pan-American Games. *Bound.-Layer Meteor.*, **166**, 113 -135.

739 Martin, J. E., 2006: *Mid-Latitude Atmospheric Dynamics: A First Course.*, West Sussex: John  
740 Wiley & Sons, 324 pp.

741 Mastrantonio, G., A. P. Viola, S. Argentini, G. Fiocco, L. Giannini, L. Rossini, G. Abbate, R.  
742 Ocone, and M. Casonato, 1994: Observations of sea breeze events in Rome and the  
743 surrounding area by a network of Doppler sodars. *Bound.-Lay. Meteor.*, **71**, 67 – 80.

744 Miller, S. T. K., B. D. Keim, R. W. Talbot, and H. Mao, 2003: Sea breeze: Structure, forecasting,  
745 and impacts. *Rev. Geophys.*, **43**, doi: 10.1029/2003RG000124.

746 Pearson, G., F. Davies, and C. Collier, 2009: An analysis of the performance of the UFAM pulsed  
747 Doppler lidar for observing the boundary layer. *J. Atmos. Oceanic Technol.*, **26**, 240 –  
748 250.

749 Prakash, J. W. J., R. Ramachandran, K. N. Nair, K. S. Gupta, and P. K. Kunhikrishnan, 1992: On  
750 the structure of sea-breeze fronts observed near the coastline of Thumba, India. *Bound.-*  
751 *Lay. Meteor.*, **59**, 111-124.

752 Rotunno, R. On the linear theory of the land and sea breeze. *J. Atmos. Sci.*, **40**, 1999 – 2009.

753 Schwab, D. J., G. A. Keshkevich, and G. C. Muhr, 1999: Automated mapping of surface water  
754 temperature in the Great Lakes. *J. Great Lakes Res.*, **25**, 468 – 481.

755 Scott, R. W. and F. A. Huff, 1996: Impacts of the Great Lakes on regional climate conditions. *J.*  
756 *Great Lakes Res.*, **22**, 845 – 863.

757 Segal, M., M. Leuthold, R. W. Arritt, C. Andersen, and J. Shen, 1997: Small lake daytime breezes:  
758 Some observational and conceptual evaluations. *Bull. Amer. Meteor. Soc.*, **78**, 1135 – 1147.

759 Shen, S., P. A. Jacques, Y. Zhu, M. D. Geller, and C. Sioutas, 2002: Evaluation of the SMPS-APS  
760 system as a continuous monitor for measuring PM<sub>2.5</sub>, PM<sub>10</sub>, and coarse (PM<sub>2.5-10</sub>)  
761 concentrations. *Atmos. Environ.*, **36**, 3939 – 3950.

762 Shipley, S. T., D. H. Tracy, E. W. Eloranta, J. T. Trauger, J. T. Sroga, F. L. Roesler, and J. A.  
763 Weinman, 1983: A High Spectral Resolution Lidar to measure optical scattering properties  
764 of atmospheric aerosols. Part I: Instrumentation and theory. *Appl. Optics*, **23**, 3716 – 3724.

765 Sills, D. M., J. R. Brook, I Levy, P. A. Makaer, J. Zhang, and P. A. Taylor, 2011: Lake breezes in  
766 the southern Great Lakes region and their influence during BAQS-Met 2007. *Atmos.*  
767 *Chem. Phys.*, **11**, 7955 – 7973.

768 Simpson, J. E., 1994: *Sea breeze and local wind*. New York: Cambridge University Press. 244  
769 pp.

770 Slade, J. H., T. M. VanReken, G. R. Mwaniki, S. Bertman, B. Stirm and P. B. Shepson, 2010:  
771 Aerosol production from the surface of the Great Lakes. *Geophys. Res. Let.*, **37**, L18807.

772 Smirnov, A., B. N. Holben, T. F. Eck, O. Dubovik, and I. Slutsker, 2000. Cloud-screening and  
773 quality control algorithms for the AERONET database. *Remote Sens. Environ.*, **73**, 337-  
774 349.

775 Stanier, C. O. and coauthors, 2021: Overview of the Lake Michigan Ozone Study 2017. *Bull.*  
776 *Amer. Meteor. Soc.*, available in early online release.

777 Turner, D.D., R. O. Knuteson, H. E. Revercomb, C. Lo, and R. G. Dedecker, 2006: Noise  
778 reduction of Atmospheric Emitted Radiance Interferometer (AERI) observations using  
779 principal component analysis. *J. Atmos. Oceanic Technol.*, **23**, 1223 – 1238.

780 Turner, D. D. and U. Löhnert, 2014: Information content and uncertainties in thermodynamic  
781 profiles and liquid cloud properties retrieved from the ground-based Atmospheric Emitted  
782 Radiance Interferometer (AERI). *J. Appl. Meteor. Climatol.*, **53**, 752 -771

783 Turner, D. D. and U. Löhnert, 2021: Ground-based temperature and humidity profiling:  
784 Combining active and passive remote sensors. *Atmos. Meas. Tech.* Accepted for  
785 publication.

786 Turner, D. D. and W. G. Blumberg, 2019: Improvements to the AERIoe thermodynamic profile  
787 retrieval algorithm. *IEEE J. Sel. Topics. Appl. Earth Observ. Remote Sens.* In press.

788 Vermeuel, M. P. and coauthors, 2019: Sensitivity of ozone production to NO<sub>x</sub> and VOC along  
789 the Lake Michigan coastline. *J. Geophys. Res Atmospheres*, **124**, doi:10.1029/  
790 2019JD030842

791 Wagner, T. J., D. D. Turner, and P. M. Klein, 2019: A new generation of ground-based mobile  
792 platforms for active and passive profiling of the atmospheric boundary layer. *Bull. Amer.*  
793 *Meteor. Soc.*, **100**, 137 – 153.

794 Wagner. T. J., W. F. Feltz, and S. A. Ackerman, 2008: The temporal evolution of convective  
795 indices in storm-producing environments. *Wea. Forecasting*, **23**, 786 – 794.

796 Xian, Z. and R. A. Pielke, 1991: The effects of width of land masses on the development of sea  
797 breezes. *J. Appl. Meteor.*, **30**, 1280 – 1304.

798 Yang, X., 1991: A study of nonhydrostatic effects in idealized sea breeze systems. *Boundary-*  
799 *Layer Meteor.*, **54**, 183 – 208.

800

801

802

803

804 **Tables**

805 Table 1: Summary of the instrumentation deployed at the two ground sites used in this study. All

806 data used in this study are publicly available at <https://www-air.larc.nasa.gov/missions/lmos/>

807

<b>Instrument</b>	<b>Deployment Site</b>	<b>Observation type</b>	<b>Approximate Vertical range</b>	<b>Temporal resolution</b>	<b>Uncertainty</b>
AERI	Sheboygan	Profiles of temperature, water vapor	0 – 3000 m	2 min	0.9 K, 1.0 g kg <sup>-1</sup>
Doppler lidar	Sheboygan	Wind vector profiles	140 – 1200 m	1.75 min	0.4 m s <sup>-1</sup>
HSRL	Sheboygan	Aerosol backscatter profiles	55 – 14600 m	0.5 min	5% of observed value
Microwave radiometer	Zion	Profiles of temperature, water vapor	0 – 3000 m	3 min	1.6 K, 1.4 g kg <sup>-1</sup>
Sodar	Zion	Wind vector profiles	30 – 200 m	2 min	0.5 m s <sup>-1</sup> , 2°
Met One AIO	Zion	Temperature, humidity, wind	10 m	1 min	0.2 K, 3% RH, 0.5 m s <sup>-1</sup>

SMPS-APS	Zion	Aerosol size distributions	5 m	20 s – 135 s	20% of aerosol diameter
Vaisala WXT 530	Sheboygan	Temperature, humidity, wind	10 m	1 min	0.3 K, 3% RH, 3% wind speed.
AERONET	Zion	Aerosol Optical Depth	Total Column	Variable	$\pm 0.1$

808

809

810 **Table 2**

811 Dates and times of the identified lake breeze events for the two observation sites during LMOS  
 812 2017 as well as lake temperatures from the GLSEA analysis. Times are in UTC; local time is UTC  
 813 – 5 and local standard time is UTC – 6. Temperatures are in °C. Blanks represent days during  
 814 which a lake breeze was observed at only one location. Times that have been bolded represent  
 815 events with inland penetration.

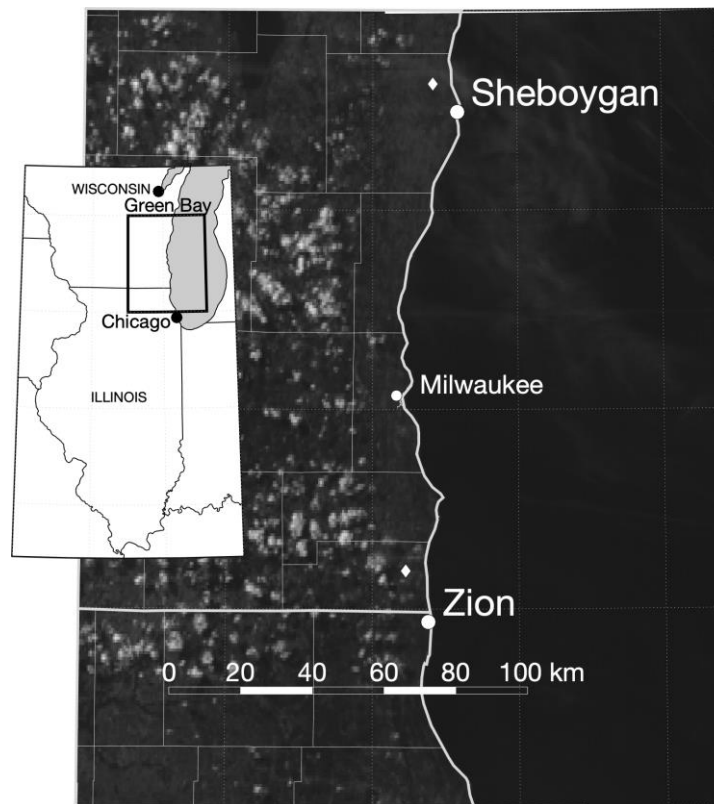
816

Date	Time at Sheboygan	Time at Zion	Sheboygan Lake Temperature (°C)	Zion Lake Temperature (°C)
2 June 2017	<b>15:42</b>	<b>14:48</b>	9.9	11.8
8 June 2017	<b>14:49</b>	<b>15:16</b>	10.9	13.1
11 June 2017	<b>14:32</b>	17:52	12.1	15.0
12 June 2017	15:43	17:30	12.1	16.1
15 June 2017	--	<b>17:20</b>	--	17.4
16 June 2017	<b>17:41</b>	17:04	14.5	17.3
17 June 2017	<b>14:20</b>	--	14.5	--

817

818 **Figures**

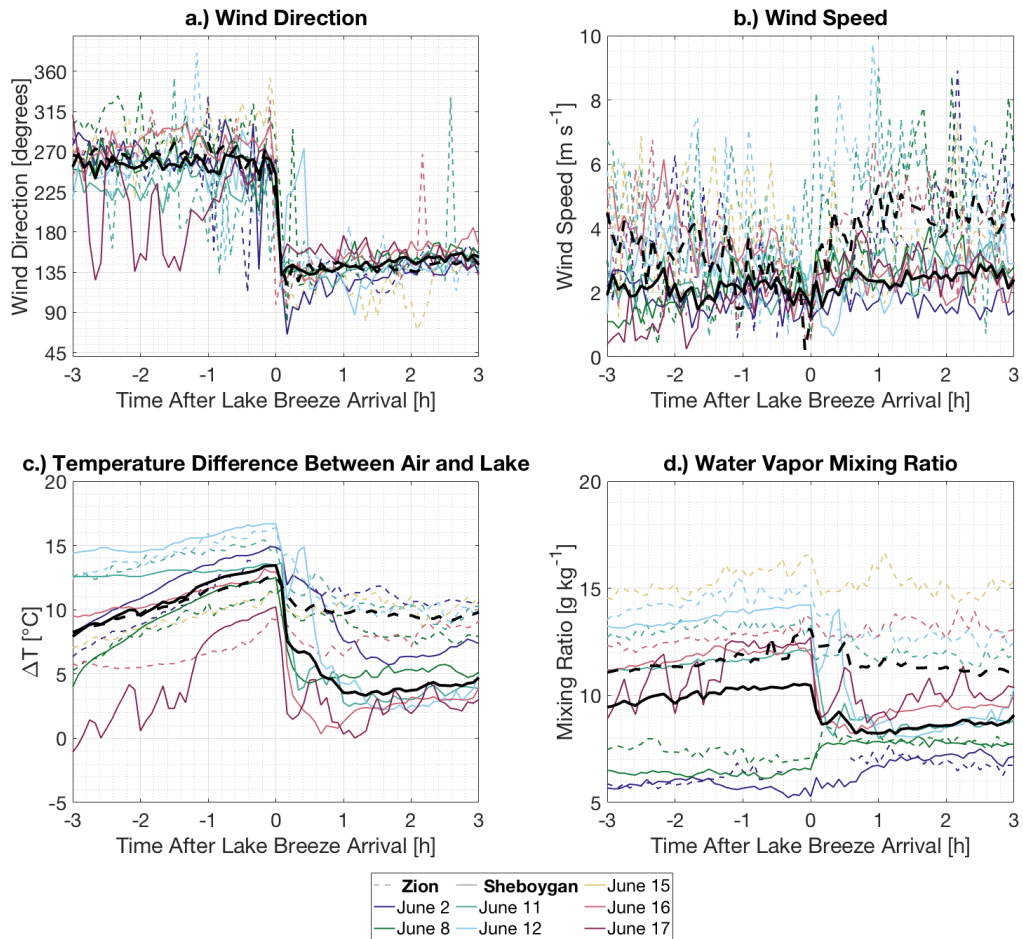
819



820

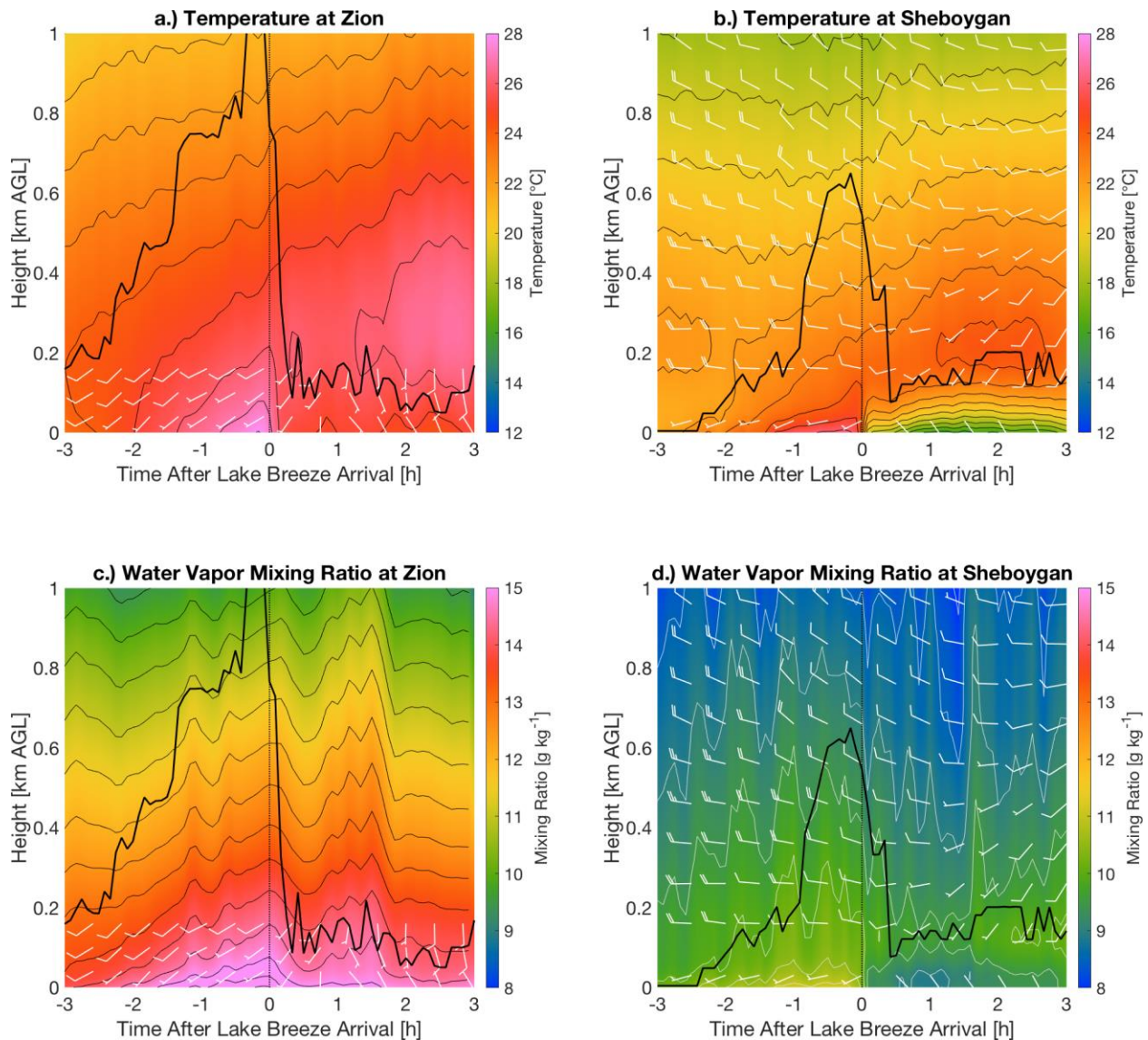
821 **Figure 1.** Location of the Sheboygan and Zion supersites along the shore of Lake Michigan,  
822 overlaid on GOES-16 0.64  $\mu\text{m}$  reflectance from 2112 UTC on 2 June 2017. Small white diamonds  
823 indicate the location of inland monitoring sites used to determine lake breeze penetration. The  
824 cities of Chicago, Illinois; and Milwaukee and Green Bay, Wisconsin, are shown for reference.  
825 The satellite imagery depicts the lack of convective clouds adjacent to the lake shore frequently  
826 seen with mature lake breezes.

827



828

829 **Figure 2.** Time series of composited surface conditions for the lake breeze events analyzed in the  
 830 present study, including a.) wind direction, in degrees; b.) wind speed, in  $\text{m s}^{-1}$ ; c.) the difference  
 831 between the air temperature and the lake surface temperature as obtained from the GLSEA  
 832 analysis, in  $^{\circ}\text{C}$ ; and d.) the water vapor mixing ratio, in  $\text{g kg}^{-1}$ . Observations from Zion are depicted  
 833 with a dashed line while observations from Sheboygan are shown with a solid line. The thick black  
 834 lines represent the mean for each site.



835

836

837

838

839

840

841

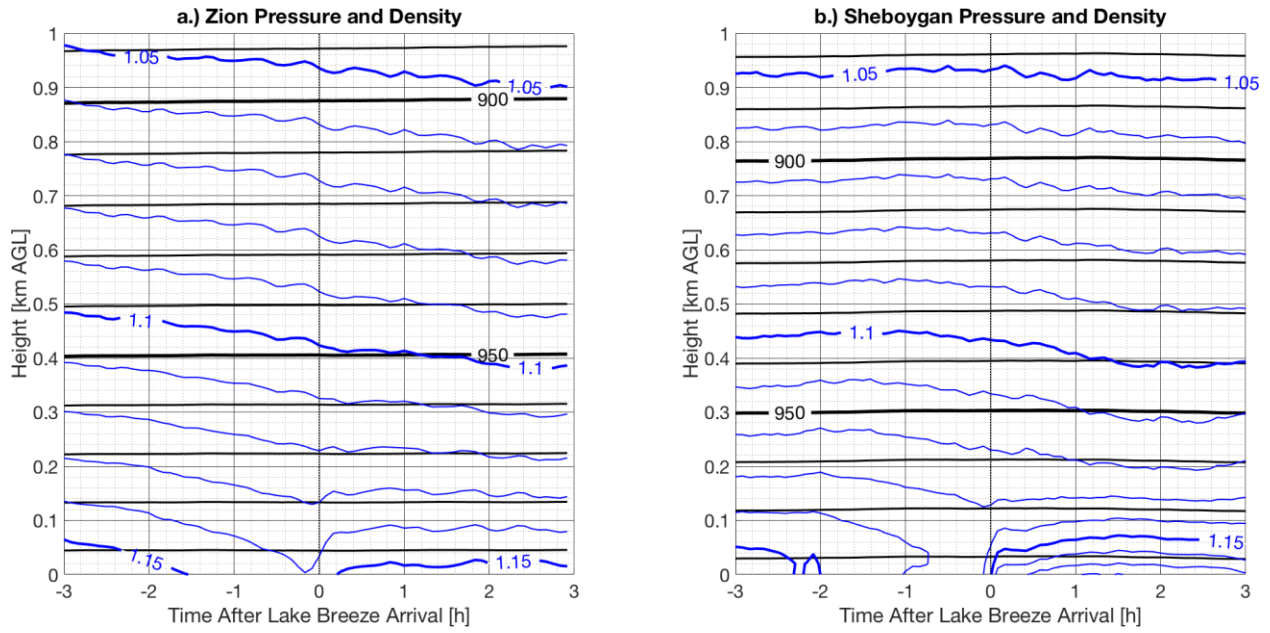
842

**Figure 3.** Time-height cross sections of temperature (top row, in  $^{\circ}\text{C}$ ) and mixing ratio (bottom row, in  $\text{g kg}^{-1}$ ) for the microwave radiometer at Zion (left column) and the AERI at Sheboygan (right column). Winds observed by the sodar at Zion and the Doppler lidar at Sheboygan are overlaid on the respective plots. Winds are shown in kt using the standard convention; this unit was chosen over  $\text{m s}^{-1}$  so that wind speed magnitudes would be large enough to be displayed with wind barbs. The 10 m surface winds at Sheboygan are appended at the bottom of the plot, but are displaced to the 30 m height for easier viewing. Temperature (mixing ratio) contours are every 1

843 °C ( $0.5 \text{ g kg}^{-1}$ ). The thick black line represents the mixing depth calculated from the  
844 thermodynamic profiles.

845

846



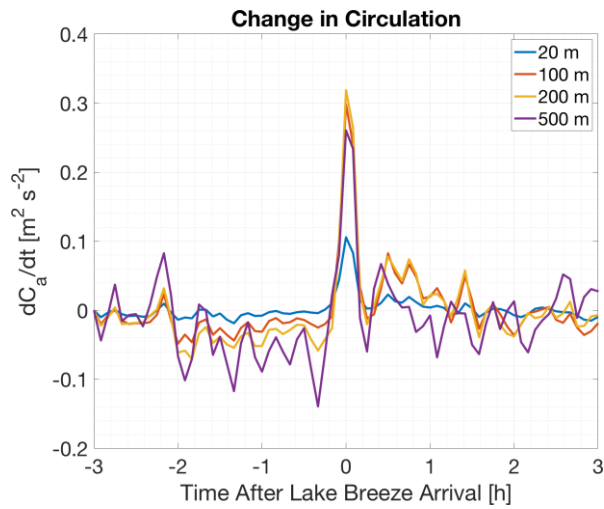
847

848

849 **Figure 4.** Time height cross sections of the mean pressure (black contours, in hPa) and density  
850 (blue contours, in kg m<sup>-3</sup>) for Zion (left) and Sheboygan (right). Pressure contours are drawn  
851 every 50 hPa and density contours are drawn every 0.05 kg m<sup>-3</sup>.

852

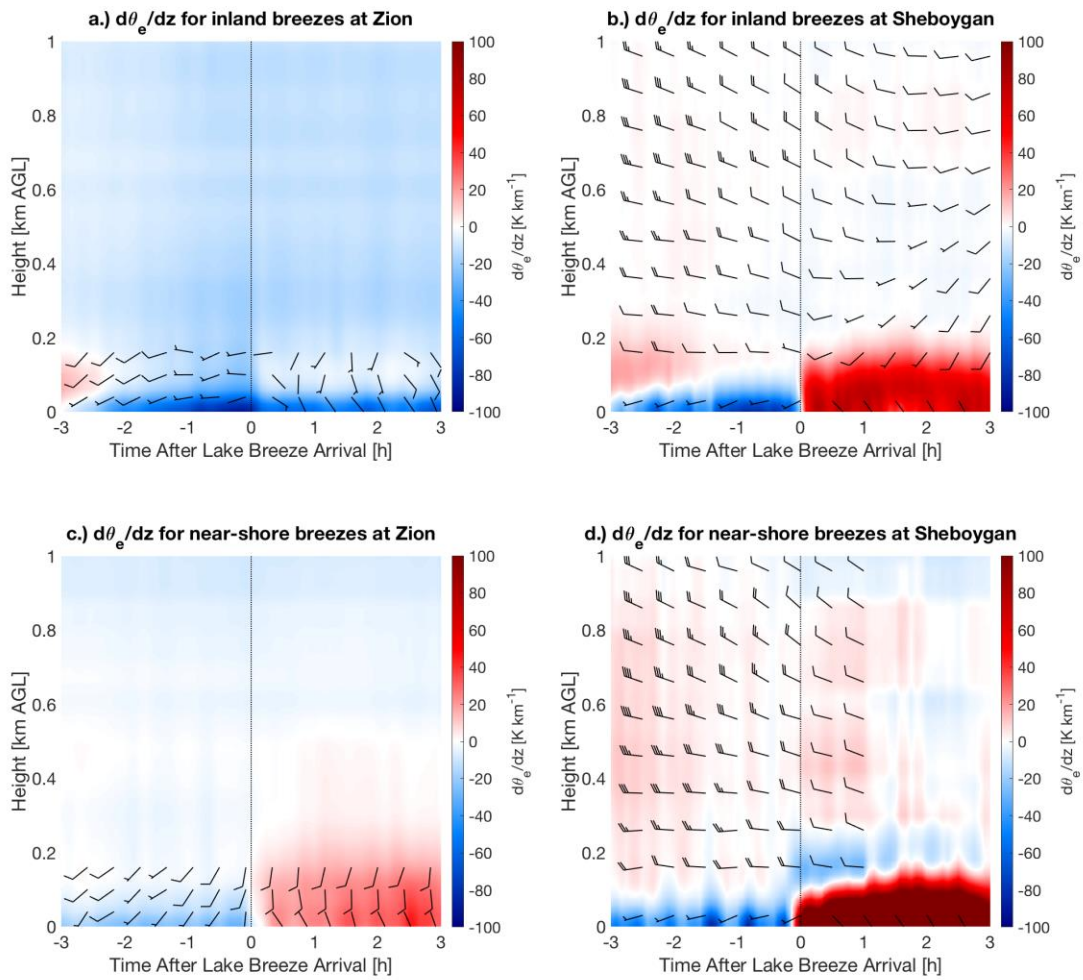
853



854

855 **Figure 5.** Time series of the temporal rate of change in circulation as derived from AERI  
 856 thermodynamic profiles. The circulation is evaluated over a layer that extends from the surface  
 857 to the listed height.

858



859

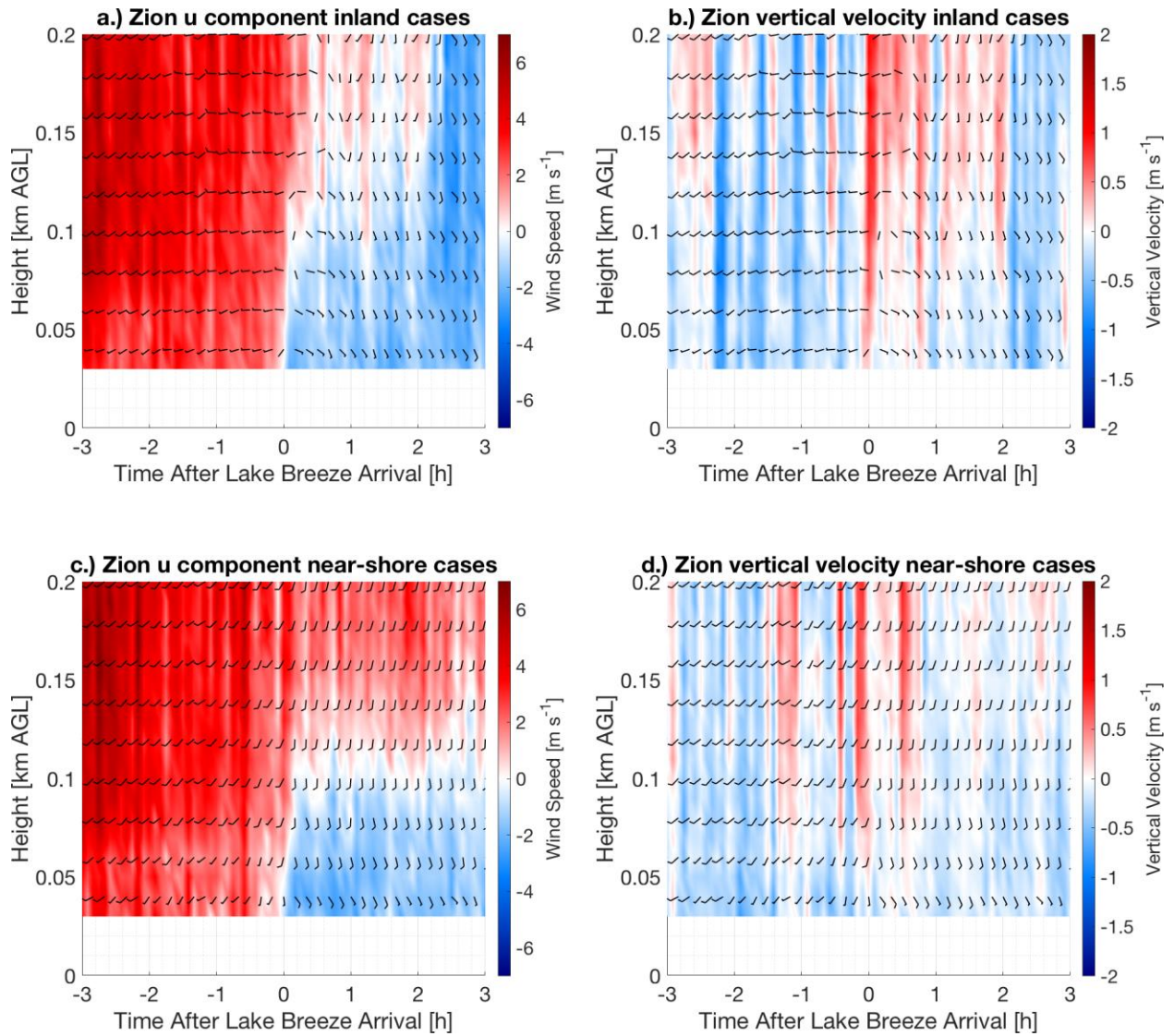
860 **Figure 6.** Time/height cross sections of the vertical rate of change of the equivalent potential

861 temperature  $\theta_e$  for inland breezes (top row) and near-shore breezes (bottom row) at Zion (left

862 column) and Sheboygan (right column). Winds follow the same plotting convention as in Figure

863 3.

864



865

866

**Figure 7.** Time/height cross sections of the sodar-observed zonal (u) wind component (left

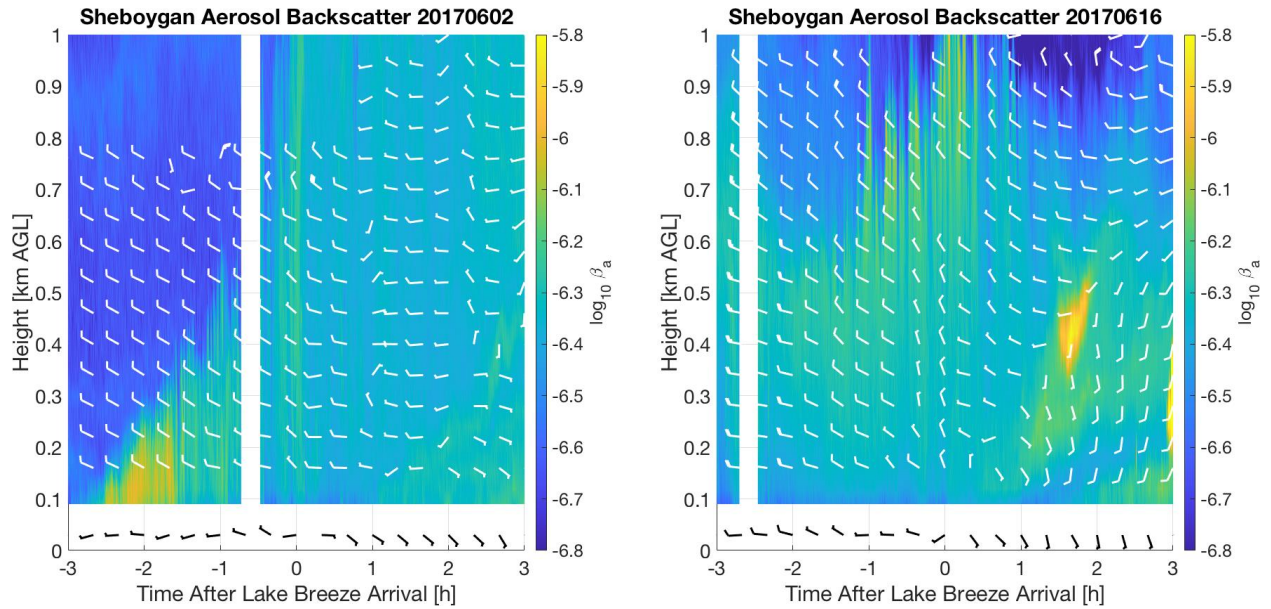
867

column) and vertical velocity (right column) at Zion for inland (top row) and near-shore (bottom

868

row) lake breezes. Wind barbs are the two dimensional horizontal wind vector, in kts.

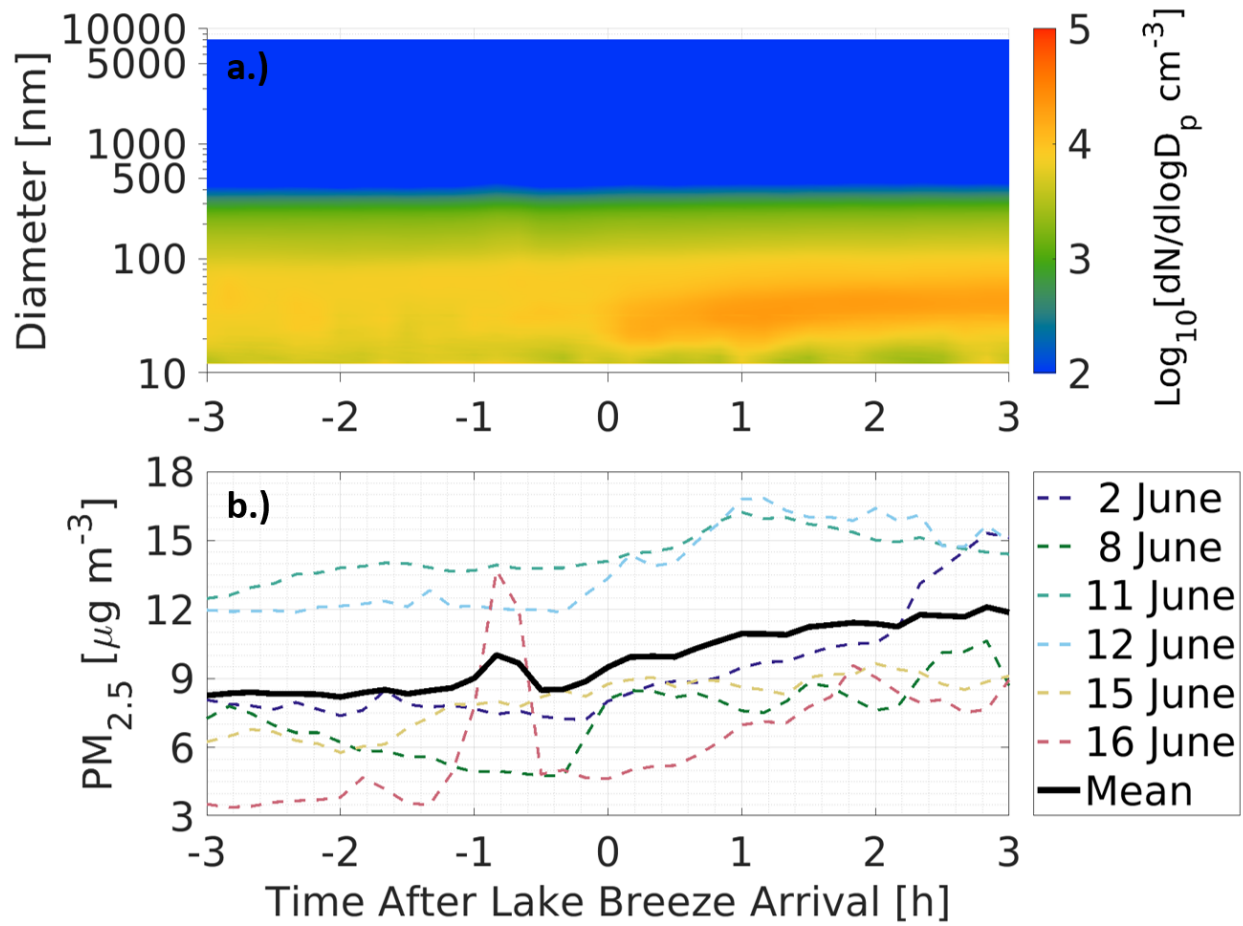
869



870

871 **Figure 8.** Time/height cross section of aerosol backscatter for two lake breeze cases from the  
 872 High Spectral Resolution Lidar (HSRL) deployed at Sheboygan. White wind barbs are from the  
 873 collocated Doppler lidar; black wind barbs are from the 10 m surface wind sensor but are plotted  
 874 at 30 m to enhance readability. Wind barbs are in kts.

875



876

877 **Figure 9.** a.) Average aerosol size distribution of all lake breeze days (in base 10 logarithm of  
 878  $\text{cm}^{-3}$ ). b.) Time series of calculated  $\text{PM}_{2.5}$  concentration (in  $\mu\text{g m}^{-3}$ ) relative to lake breeze arrival  
 879 time.